


7-31-2017

DNA Analysis of Surfactant-Associated Bacteria in a Natural Sea Slick in the Gulf of Mexico Observed by TerraSAR-X

Kathryn Howe

Nova Southeastern University, kh1271@nova.edu

Follow this and additional works at: https://nsuworks.nova.edu/occ_stuetd

 Part of the [Marine Biology Commons](#), and the [Oceanography and Atmospheric Sciences and Meteorology Commons](#)

Share Feedback About This Item

NSUWorks Citation

Kathryn Howe. 2017. *DNA Analysis of Surfactant-Associated Bacteria in a Natural Sea Slick in the Gulf of Mexico Observed by TerraSAR-X*. Master's thesis. Nova Southeastern University. Retrieved from NSUWorks, . (451)
https://nsuworks.nova.edu/occ_stuetd/451.

This Thesis is brought to you by the HCNSO Student Work at NSUWorks. It has been accepted for inclusion in HCNSO Student Theses and Dissertations by an authorized administrator of NSUWorks. For more information, please contact nsuworks@nova.edu.

HALMOS COLLEGE OF NATURAL SCIENCES AND OCEANOGRAPHY

DNA analysis of surfactant-associated bacteria in a natural sea
slick in the Gulf of Mexico observed by TerraSAR-X

By:

Kathryn Lynn Howe

Submitted to the Faculty of
Halmos College of Natural Sciences and Oceanography
in partial fulfillment of the requirements for
the degree of Master of Science with a specialty in:

Coastal Zone Management

Nova Southeastern University

July 2017

Table of Contents

List of figures.....	3
List of tables.....	5
Acknowledgements.....	6
Abstract	7
1. Introduction.....	8
a. Natural sea slicks.....	8
b. Bacteria.....	8
c. Sea surface microlayer.....	9
d. Remote sensing.....	10
e. DNA analysis	12
i. Real time PCR.....	12
ii. Sequencing.....	14
f. Previous work.....	15
2. Objectives.....	17
a. Significance.....	17
b. Hypotheses.....	18
3. Materials, methods, and measurements.....	18
a. Locations.....	18
b. Sample collection.....	19
c. DNA Analysis.....	22
i. DNA extraction.....	22
ii. Real time PCR.....	22
iii. Sequencing.....	23
4. Results and discussion.....	24
a. SAR overpass.....	24
b. qPCR results.....	25
i. LASER 2016.....	25
ii. SCOPE 2013.....	28
c. Sequencing results.....	29
i. LASER 2016.....	29
ii. SCOPE 2013.....	40
iii. Contamination.....	40
5. Conclusions.....	41
6. References.....	43

Supplementary Material

List of Figures

Figure 1: SAR signal scattering	11
Figure 2: PCR mechanism	13
Figure 3: qPCR plot	14
Figure 4: LASER 2016 sampling locations	21
Figure 5: SAR results LASER 2016	25
Figure 6: LASER 2016 qPCR results	27
Figure 7: SCOPE 2013 qPCR results for 12/11/13	28
Figure 8: SCOPE 2013 qPCR results for 12/16/13	29
Figure 9: LASER 2016 and SCOPE 2013 relative abundance by sequencing	30
Figure 10: Total OTU hits per site	31
Figure 11: Average <i>Bacillus</i> OTU hits.....	32
Figure 12: Average <i>Pseudomonas</i> OTU	33
Figure 13: Average <i>Corynebacterium</i> OTU hits	34
Figure 14: Average <i>Acinetobacter</i> OTU hits	35
Figure 15: Average <i>Marinobacter</i> OTU hits	35
Figure 16: Average <i>Rhodococcus</i> OTU hits	36
Figure 17: Average <i>Halomonas</i> OTU hits	36
Figure 18: Average <i>Micrococcus</i> OTU hits	37
Figure 19: Average <i>Mycobacterium</i> OTU hits	38
Figure 20: Average <i>Arthrobacter</i> OTU hits	39
Figure 21: Average <i>Enterobacter</i> OTU hits	39
Figure 22: Average Other/unassigned OTU hits per site, including NE controls, after removing surfactant-associated bacteria.	40
Figure S1: Relative abundance of surfactant-associated bacteria of each sample in Site 2.....	47
Figure S2: Relative abundance of surfactant-associated bacteria of each sample in Site 3	48

Figure S3: Relative abundance of surfactant-associated bacteria of each sample in Site 4	48
Figure S4: Relative abundance of surfactant-associated bacteria of each sample in Site 5	49
Figure S5: Relative abundance of surfactant-associated bacteria of each sample in Site 6	49
Figure S6: Relative abundance of surfactant-associated bacteria of each sample in Site 7	50
Figure S7: Relative abundance of surfactant-associated bacteria of each sample in Site H_11.....	51
Figure S8: Relative abundance of surfactant-associated bacteria of each sample in Site H_12	52
Figure S9: Relative abundance of surfactant-associated bacteria of each sample in Site H_13	53

List of Tables

Table 1: Bacteria and their surfactant-association and oil- association	9
Table 2: SCOPE 2013 data table	16
Table 3: LASER 2016 data table.....	21
Table 4: qPCR efficiencies	26
Table S1. <i>Bacillus</i> absolute abundance with Poisson distribution	54
Table S2. <i>Pseudomonas</i> absolute abundance with Poisson distribution	54
Table S3. <i>Corynebacterium</i> absolute abundance with Poisson distribution	55
Table S4. <i>Acinetobacter</i> absolute abundance with Poisson distribution	55
Table S5. <i>Marinobacter</i> absolute abundance with Poisson distribution	56
Table S6. <i>Rhodococcus</i> absolute abundance with Poisson distribution	56
Table S7. <i>Halomonas</i> absolute abundance with Poisson distribution	57
Table S8. <i>Micrococcus</i> absolute abundance with Poisson distribution	57
Table S9. <i>Mycobacterium</i> absolute abundance with Poisson distribution	58
Table S10. <i>Arthrobacter</i> absolute abundance with Poisson distribution	58
Table S11. <i>Enterobacter</i> absolute abundance with Poisson distribution	59
Table S12. Other/unassigned absolute abundance with Poisson distribution	59

Acknowledgements

I thank my major advisor, Dr. Alexander Soloviev, for the opportunity to conduct and present this research, both domestically and internationally. Thank you to my committee members for their guidance and support. Thank you to Dr. Mahmood Shivji's lab, especially Kim Finnegan, Dr. Andrea Bernard, Cassandra Ruck, Cristin Fitzpatrick for help with Illumina library preparation protocol and general lab procedures. Thank you to Dr. Aurelien Tartar for use of his lab and guidance with qPCR methodology. Thank you to Dr. Brian Haus for contributions to the final paper and organization of sample collection during the LASER experiment in the Gulf of Mexico. I am grateful to Dr. Susanne Lehner (DLR) and Will Perrie (BIO) for collection of SAR imagery and to Cayla Dean and John Kluge for help with sample collection. Thank you to Dr. Cole Easson and Jorie Skutas for assistance with QIIME and downstream data analysis.

This thesis work was supported by the Gulf of Mexico Research Initiative (GoMRI), the Consortium for Advanced Research on Transport of Hydrocarbon in the Environment (CARTHE). Travel support was partially funded by the Oceanographic Center Student Government Association (OC SGA) travel grants and a National Science Foundation (NSF) travel award.

Finally, I thank my parents, siblings, and friends for providing support and encouragement during my graduate studies.

Abstract

Under low wind speed conditions, surfactants accumulate at the air-sea interface, dampen short-gravity capillary (Bragg) waves, and form natural sea slicks that are detectable visually and in synthetic aperture radar (SAR) imagery. Marine organisms, such as phytoplankton, zooplankton, seaweed, and bacteria, produce and degrade surfactants during various life processes. This study coordinates *in situ* sampling with TerraSAR-X satellite overpasses in order to help guide microbiological analysis of the sea surface microlayer (SML) and associated subsurface water (SSW). Samples were collected in the Gulf of Mexico during a research cruise (LASER) in February 2016 to determine abundance of surfactant associated bacteria in the sea surface microlayer and subsurface water column. By using real-time polymerase chain reaction (quantitative PCR, or qPCR) to target *Bacillus* spp. associated with surfactant production, results indicate that more surfactant-associated bacteria reside in the subsurface water in low wind speed conditions. Sequencing results suggest that *Bacillus* and *Pseudomonas* are more abundant in the SSW in low wind speed conditions. These results indicate that these bacteria reside in the SSW, presumably producing surfactants that move to the surface via physical processes, accumulate on and enrich the sea surface microlayer.

Keywords: bacteria, synthetic aperture radar, sea surface microlayer, sequencing

1. Introduction

1a. Natural Sea Slicks

Natural sea slicks are caused by the accumulation of organic material due to the following factors: coastal blooms, high precipitation, terrestrial runoff (Wurl et al., 2011); oceanic features, such as convergence zones or frontal interfaces and internal waves (Gade et al., 2013); high biological productivity; and sediment upwelling/resuspension (Espedal and Johannessen, 1996). They are highly variable in time and space, because they can be easily disturbed by wind and wave breaking. Under low wind speed conditions, surface-active compounds (surfactants) accumulate and form natural slicks on the sea surface. Slicks are detectable visually due to their glossy appearance and in synthetic aperture radar (SAR) imagery due to their wave-damping properties. The presence of surfactants and sea slicks has an effect on the rate of gas exchange at the air-sea interface (Soloviev and Lukas 2014) and may have implications on other biogeochemical processes as well.

1b. Bacteria

Bacteria are vital to life on this planet. They are the basis of the food web, responsible for recycling nutrients and trace elements. Bacteria are essential to ocean function by being a critical link in the ocean's carbon cycle by producing/consuming greenhouse gases among others (Karl 2007). There is an estimated 3.67×10^{30} microorganisms in the marine environment, yet less than 0.1% are known (Whitman et al. 1998), because most marine microbes cannot be cultured in a laboratory (Amann et al. 1995).

Some marine bacteria produce surfactants, which are composed of glycolipids, lipopeptides, phospholipids, exopolysaccharides, and other complex compounds (Satpute et al. 2010). Surfactants are amphiphiles that have a hydrophobic and a hydrophilic end, and can therefore span the air-sea interface. When surfactants accumulate on the sea surface under low wind speed conditions, they dampen of short-gravity capillary (Bragg) waves (Gade et al. 2013).

Surfactant-associated bacterial genera include surfactant producers such as *Bacillus*, *Corynebacterium*, *Acinetobacter*, *Enterobacter*, *Halomonas*, *Rhodococcus*, *Marinobacter*, *Micrococcus*, *Mycobacterium*, and *Arthrobacter* and degraders, including *Pseudomonas* (also a surfactant-producer) (Abraham et al. 1998; Maeerate et al. 2006; Perfumo et al. 2006; Satpute et al 2010). Bacteria produce and utilize surfactants for food capture, motility, hydrocarbon degradation, toxin isolation, as a nutrient source (Dinamarca 2013), as well as protection and aggregation (Sayem et al. 2011; Kurata 2012). One function of surfactants is the breakdown of hydrocarbons such as natural gas and oil. Table 1 shows well-known surfactant-associated bacterial genera. All of the bacterial genera shown in Table 1 also include species of oil-degrading bacteria (Brooijmans et al. 2009).

Table 1. Bacteria and their surfactant-association and oil association. Table of several bacterial genera that produce/degrade surfactants and contain oil-degrading species (Abraham et al. 1998; Harayama et al. 2004; Brooijmans et al. 2009; Satpute et al. 2010; Dinamarca et al. 2013).

Genus	Surfactant association	Oil association
<i>Pseudomonas</i>	Producer and degrader	Degrader
<i>Enterobacter</i>	Producer	Degrader
<i>Arthrobacter</i>	Producer	Degrader
<i>Mycobacterium</i>	Producer	Degrader
<i>Micrococcus</i>	Producer	Degrader
<i>Halomonas</i>	Producer	Degrader
<i>Rhodococcus</i>	Producer	Degrader
<i>Marinobacter</i>	Producer	Degrader
<i>Acinetobacter</i>	Producer	Degrader
<i>Corynebacterium</i>	Producer	Degrader
<i>Bacillus</i>	Producer	Degrader

1c. Sea Surface Microlayer

The sea surface microlayer (SML) is a known accumulation zone for many compounds including surfactants, proteins, polysaccharides, and other complex compounds (Cunliffe et al. 2011). Historic models of the SML show a highly stratified environmental structure, where there is an upper layer of lipids, fatty acids, and alcohols, over a layer of proteins and polysaccharides which extends into the subsurface water (Hardy 1982). Other models depict the SML as a heterogeneous mixture of gel-like particles and bacteria (Cunliffe et al. 2011).

The SML is considered an extreme environment due to the drastic fluxes in temperature, salinity, pH, nutrients, and radiation (solar and UV) (Maki 1993). Fluctuating physical and chemical factors, such as atmospheric deposition, turbulent mixing, seasonality, trophic state, organic pollutants, heavy metals, and UV radiation, can all influence slick and microbial community structure (Karl 2007; Stolle et al 2010). The SML may influence biogeochemical processes at the air-sea interface, such as heat and gas exchange (Liss and Duce, 1997), particle cycling (Wheeler 1975; Wurl and Holmes 2008) and microbial loops (Reinthal et al. 2008). The microlayer has exchanges with both the subsurface water (SSW) and atmosphere. Wind affects the supply and removal processes in the SML, which adds to the spatial and temporal variability of sea slicks and microbial communities (Stolle et al. 2010)

1d. Remote Sensing

Satellite imagery is used for monitoring agriculture and urban development, oil spill detection, natural disaster response, military surveillance, and many other applications. The use of synthetic aperture radar (SAR) imagery has become increasingly popular for imaging coastal and oceanographic features. Features such as internal waves, ship wakes, oil spills, wind shadows, grease ice, convergence zones, and biogenic slicks can be visible in SAR imagery (Gade et al. 2013). Information such as wave spectra, wind field, and ocean currents can be extracted from SAR images using specific algorithms. *In situ*

measurements greatly help remote sensing specialists to understand why certain features are visible in order to develop better algorithms for the interpretation of these images. With an increasing number of SAR satellites, SAR images are gradually becoming more readily available to the scientific community at little to no cost.

The electromagnetic waves emitted by SAR satellites scatter depending on the surface being imaged. Rough surfaces send a high amount of backscatter to the receiving antenna and appear as bright areas in a SAR image, while smooth surfaces reflect a low amount of backscatter in the direction of the antenna and appear as dark areas in the image (Figure 1). Different SAR satellites utilize various wavelengths and ranges of incidence angles in order to image a surface, allowing for different views of the same feature. For example, TerraSAR-X works in X-band range, which has a wavelength range of 2.5-4 cm wavelengths. RADARSAT-2, a C-band sensor, has a wavelength range of 4-8 cm (<http://www.esa.int>).



Figure 1. SAR signal scattering. A) A rough surface reflects most of the radar signal back to the receiving antenna, while a smooth surface (B) reflects the signal away from the receiving antenna. From Liew (2001).

The advantage of SAR satellites is that they can image surfaces without the constraint of sunlight and are able to penetrate fog and cloud cover. The main challenges of SAR satellite imagery involve scheduling the satellite overpass coordinated with *in situ* measurements. In this study, there was approximately a 25%-33% success rate of sampling in the scheduled satellite footprint during the overpass. Contributing factors

were as follows: adverse weather conditions, conflicting schedules for the use of the research vessel, cancellations of SAR satellite imagery at the last moment due to higher priority users. Another challenge is the interpretation of SAR images. Coordinated *in situ* measurements provide invaluable information for the interpretation.

1.e. DNA Analysis

1.e.i. Real time Polymerase Chain Reaction

In studies, such as this one, that have small amount of starting DNA, techniques are required in order to amplify that DNA to amounts in which it can be studied. Real-time polymerase chain reaction (quantitative PCR, or qPCR) is a technique used to amplify a predetermined sequence of DNA over a billion-fold, while monitoring the amplification in real time by measuring fluorescence. This method requires DNA polymerases, sequence primers, and a fluorescent dye (SYBR green I) and involves the repeated heating and cooling of the reaction mixture. The first step of qPCR is initialization, where the temperature is raised in order to activate polymerases and denature the template DNA. After initialization, the cycle including denaturation, annealing, and elongation, is repeated up to 35 times. An increase of cycles over 35 can lead to nonspecific amplification and other errors (<http://www.biom-rad.com>). Within the cycle, primers and DNA polymerases anneal to single-stranded DNA according to their target sequence. Elongation occurs when DNA polymerases copy the single-stranded DNA and copy it in the 3' – 5' direction (Figure 2).

When the new double-stranded DNA copy (amplicon) forms, SYBR green I binds in the minor groove of the amplicon and fluoresces; this fluorescence is measured after every cycle. The more target DNA present, the more fluorescence is produced by SYBR green I. However, SYBR green is sequence-independent, meaning that it can bind to any newly formed double-stranded DNA, even if it is not the target sequence, and cause a false fluorescence (Ponche et al. 2003). False fluorescence can be inferred from melt curve analysis.

After all cycles have finished, a corrected amplification plot (Figure 3) with background fluorescence removed, is generated. Figure 3 shows cycle number on the x-axis and fluorescence on the y-axis. A threshold is automatically or manually set in the linear phase of amplification. The cycle number where a sample, represented by a single line, crosses this threshold is called the CT value. The CT value is used to compare abundances of target DNA in each sample.

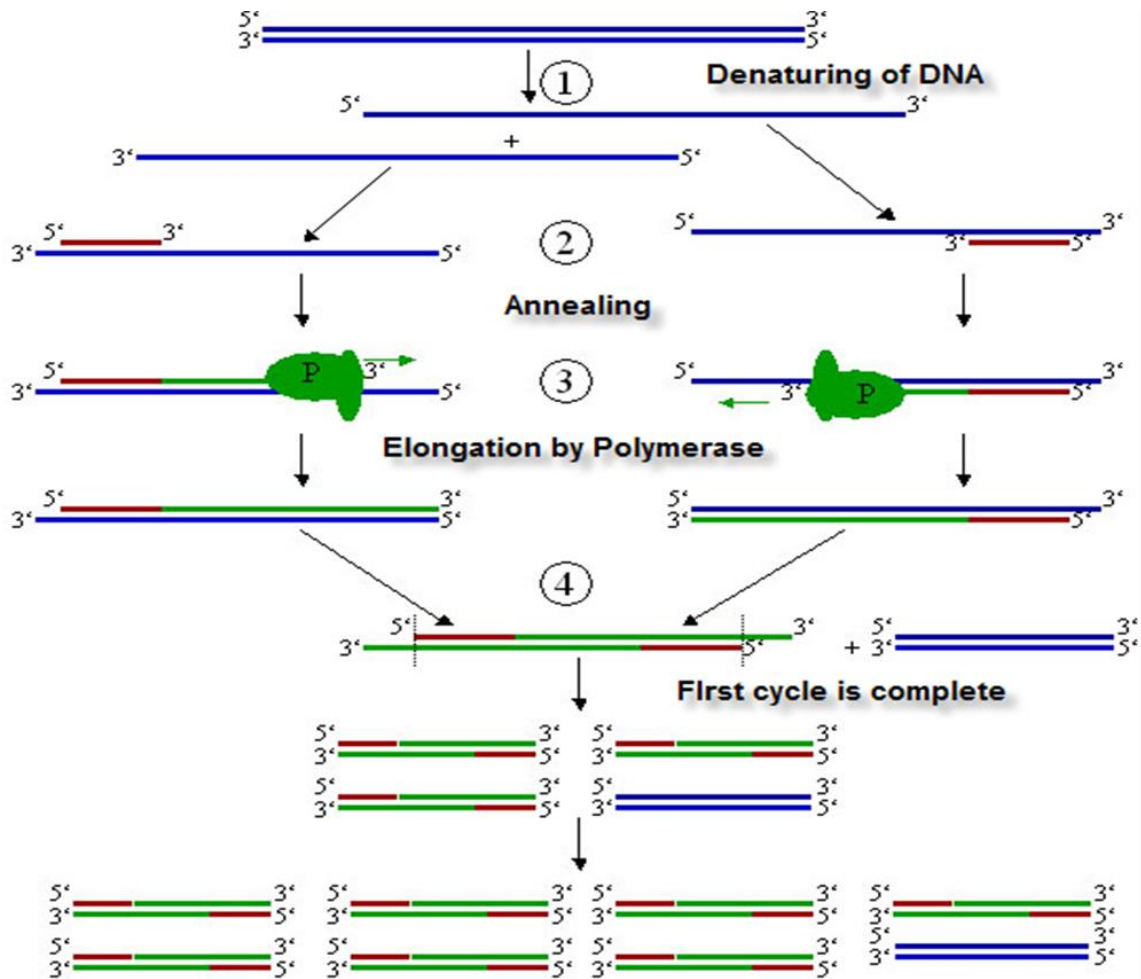


Figure 2. PCR mechanism. Schematic showing the main steps of PCR: denaturation, annealing, and elongation.

(https://serc.carleton.edu/microbelife/research_methods/genomics/pcr.html)

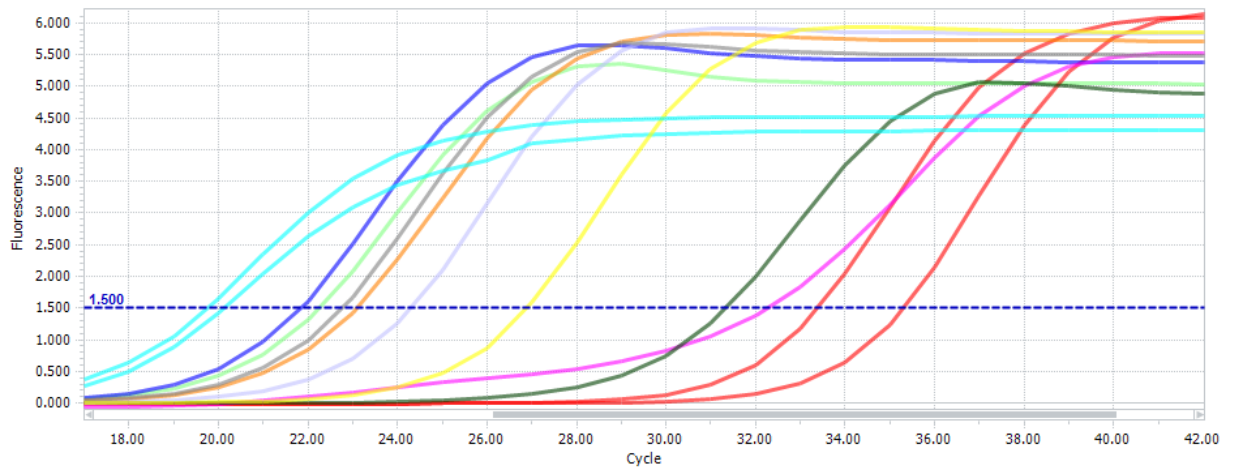


Figure 3. qPCR plot. This qPCR amplification plot shows the positive controls (bright blue), negative controls (red), SSW samples (dark blue, light green), SML samples (gray, orange, light purple, yellow, dark green), and an air control (bright pink) from Site 3. The CT values corresponding with the threshold at 1.5 (blue dashed line) were used for abundance calculations.

1.e.ii. Sequencing

Next-generation sequencing, also known as high-throughput sequencing, has become increasingly popular due to its high efficiency and low costs (Caporaso et al 2011; Caporaso et al. 2012). Illumina sequencing by synthesis provides high accuracy and high yield of error-free reads (<http://www.illumina.com>). Illumina sequencing was used in this study to determine bacterial community composition of the SML and SSW. The 16S rRNA gene is the standard for classification and identification of microbes, because it is present in most microbes and the V3 and V4 hypervariable regions specifically show slow rates of evolution (Yang et al. 2016).

Data is provided from the Illumina MiSeq interface in fastq format, which can be analyzed using a variety of bioinformatics software, such as QIIME (Quantitative Insights Into Microbial Ecology). Illumina MiSeq sequencing provides genus-level, and in some cases species-level, identification of bacteria through use of operation taxonomic

units (OTUs). OTUs are used to categorize bacteria based on sequence similarity. Similarity is typically defined at a 97% threshold of the 16S gene sequence variants at genus level. Standard OTUs are determined by Greengenes, which is a 16S reference database based on a *de novo* phylogeny (McDonald et al. 2012).

1.f. Previous work

Kurata et al. (2016) used 454 sequencing to determine microbial composition in the SML and SSW from samples collected in the Straits of Florida. Bacterial communities in slick versus non-slick conditions were distinct; *Bacillus* spp. were more abundant in slick, microlayer samples compared to non-slick, microlayer samples. In this study, there was one sample per water type and per site. However, several surfactant-associated bacteria genera were analyzed, due to the use of 454 sequencing.

Hamilton et al. (2015a and 2015b) used qPCR techniques to determine relative abundance of only one bacterial genus, *Bacillus* (which is a well-known surfactant-producing bacterial genus). Samples in this study were collected in the Gulf of Mexico and Straits of Florida. One site in the Straits of Florida had wind speeds of 3-4 m/s and results indicated a statistically significant difference between SML and SSW. The analysis showed a higher abundance of *Bacillus* spp. in the SSW of non-slick conditions (Hamilton et al. 2015a, b). Relative abundance for samples collected in the Gulf of Mexico in December of 2013 during SCOPE (Surfzone Coastal Oil Pathways Experiment) indicated that under low wind speed, slick conditions, there was a higher abundance of *Bacillus* in the SSW compared to SML (Table 2). In Hamilton et al. (2015a, b), only four samples were collected and analyzed per water type and per site, which may not be sufficient in the case of highly intermittent bacterial environments. This is the reason for increasing the number of samples in the present study.

Franklin et al. (2005) pioneered a method of sampling the sea surface microlayer with a polycarbonate membrane filter. Their results from the North Sea show that there was less bacterial diversity in the SML compared to SSW, furthering the idea that the

bacterial community composition of the SML is distinct from the SSW. Agogue et al. (2005), using the same method of sample collection as Franklin et al. (2005), analyzed the bacterial composition of the sea surface microlayer, in polluted and oligotrophic sites in the Mediterranean Sea.

Table 2. SCOPE 2013 data table.

Site	Date	Slick present	SML samples analyzed	SSW samples analyzed	Waves (m)	Wind (m/s)	Location
H_11	12/11/2013	Yes	86, 89	29, 64	0.3	1-2	Destin, FL., nearshore
H_12	12/11/2013	No	111	44	0.3	1-2	Destin, FL., nearshore
H-13	12/16/2013	Yes	110	59	<0.3	<3	Pensacola, FL., 20 mi offshore

Many other techniques have been used to sample the biological and chemical parameters in the sea surface microlayer. The various methods define the sampling depth differently, making comparisons of microbial community structure challenging. For example, a mesh screen samples from 150 – 400 μm (Sieburth 1965), compared to a glass plates that samples from 20 – 100 μm (Harvey and Burzell 1972) and hydrophilic polycarbonate filter that samples from 4 – 40 μm (Crow et al. 1975). Practical application of using mesh screens and glass plates to sample the sea surface microlayer are often associated with uncontrollable contamination from the water column or ship-induced distortions to measurements. The method using polycarbonate filters helps to overcome most of the contamination issues (Kurata et al. 2016).

2. Objectives

2.a. Significance

The SML is a vital environmental boundary and has an effect on the transfer of momentum, heat, and gas across the air-sea interface. The microbiological nature of the microlayer greatly influences exchange with the atmosphere (Cunliffe et al. 2011). Unfortunately, researchers utilizing different sampling methods cannot agree on the definition of the microlayer (which is an indication of the gravity of the problem of SML exploration). This study utilizes a hydrophilic polycarbonate filter with a 47 mm diameter, which samples the SML at a depth of 4-40 μm (Crow et al. 1975).

Certain marine organisms, including bacteria, produce surfactants for nutrient acquisition, toxin isolation, protection, and aggregation. When surfactants accumulate on the sea surface under low wind speed conditions, they form sea slicks, which are visible in SAR imagery. Surfactants may be produced in SSW and transported to the SML by advection, turbulence, wave breaking, and bubble scavenging. As a result, SAR technology can be advanced to monitor organic materials in the water column, including dissolved oil (see section 6d).

Due to extreme difficulty of measurements on submillimeter scales at the moving air-water interface, the SML is still poorly understood. There are species of marine bacteria, which have never been identified. As a result, the SML holds opportunity for discovery of new species of marine bacteria. Extinction may be occurring as well. Species could be disappearing every day and we currently have no way of measuring the loss. The lack of knowledge of species composition is exacerbated by the fact, as mentioned above, that many marine microorganisms are not culturable in the lab (Harayama et al. 2004).

The new sampling locations of this study may help establish a relationship between surfactant production and primary production, as well as provide information on

global coverage of natural sea slicks and generation of climate-related aerosol (Kurata et al. 2016).

2.b. Hypotheses

- Meteorological conditions influence microbial community structure in the near surface of the ocean.
- There is higher abundance of surfactant-associated bacteria in the SSW compared to the SML in slick conditions.
- SAR technology can be used to identify potential areas of dissolved organic material in the water column, including dissolved oil, by the presence of surface slicks associated with surfactants produced by bacteria below the water surface.

3. Materials, methods, and measurements

3.a. Locations

In this work, samples collected during a Gulf of Mexico Research Initiative (GoMRI) Consortium for Advanced Research on the Transport of Hydrocarbons in the Environment (CARTHE) Lagrangian Submesoscale Experiment (LASER) 2016 research cruise were analyzed. During three sampling days, over 100 samples were collected (Table 3). The sites on February 10 were nearshore in the brown water of the Mississippi River outflow, while the sites on February 6 and 12 were offshore, closer to the Deepwater Horizon site (Figure 4). Except for Site 1 which has been removed from the analysis, each site has both SML and corresponding SSW samples. Slick presence was determined visually and confirmed in TerraSAR-X imagery, which was provided by the German Aerospace Center (DLR). Wind speed was collected from the R.V *F.G Walton Smith*.

3.b. Sample collection

A technique developed by Franklin et al. (2005) has been advanced by researchers at Nova Southeastern University to reduce contamination by the ship's wake, boat, and researcher (Hamilton et al. 2015a, b; Kurata et al. 2016). Sterilization and contamination control is imperative in this study, especially since the focus is on bacteria. All sampling was recorded on video via GoPro camera to verify that there was no accidental contamination of the polycarbonate filter by contact with the boat, ship's wake, or researchers during deployment and recovery of the filter. Polycarbonate membrane filters, which have a sampling depth of 4-40 μm (Crow et al. 1975), were attached to a sterile hook and fishing line with a loop at the far end. The sampling apparatus was stored in a sterile bag until ready for deployment in the field. When ready to sample, the loop was attached to a swivel tied on to a ten-foot fishing pole. The pole allowed for the deployment of the filter in an area undisturbed by the ship wake. Using the pole, the filter was then lifted off the surface of the water and retrieved from the fishing line by a researcher with sterile forceps. The filter was rolled and placed in a labeled 5 mL MoBio bead tube that was used for DNA extraction. This storage technique allowed for maximum retention of the sample, which was important since the sample size was so small to begin with. Samples were held on ice in the field and transferred to a -80°C freezer where they were stored until extraction.

To sample the subsurface water, a sterilized tube was attached to a peristaltic pump and an extension pole was used to reach undisturbed area to collect water at approximately 0.2 m depth. The tube was sterilized prior to each use with isopropanol before SSW was run through the tubing for about 30 s. The sample was then collected into a sterile bag. Using sterile forceps, the filter was dipped into the bag swirled around for a few seconds. It was taken out, rolled, and placed in a labeled 5 ml MoBio bead tube. SSW samples were stored in the same method as the SML samples.

In addition, control filters were analyzed for possible contamination during handling in the field and in the lab. There were two types of control filters, which

included the filters exposed to the air (AC) and non-exposed filters (NE). AC filters were used to test for possible bacterial contamination from marine aerosols. NE filters (exposed only to the laboratory environment) were processed to detect laboratory and procedural contamination.

Slicks were detected visually and verified in SAR imagery. Wind speed was recorded on the R/V *F.G. Walton Smith*. Wind speeds below 5 m/s were considered low wind speed conditions, while winds over 5 m/s were considered moderate wind speed conditions, since that is the wind speed which induces wave breaking.

Overpasses of TerraSAR-X and RADARSAT-2 satellites were scheduled by the German Aerospace Center (DLR) and Bedford Institute of Oceanography (BIO) to coordinate with *in situ* sampling. Quick look images were provided for analysis in this study.

Samples collected in 2013 by Hamilton et al. (2015a, b) in two locations of the Gulf of Mexico as part of the CARTHE SCOPE campaign near Destin, FL (Table 2) were also included in this analysis. Eight samples from the 2013 field campaign were sent to Argonne National Laboratory (ANL) for amplification and sequencing. All of these samples were collected under low wind speed conditions (less than 3 m/s). Sites H_11 and H_13 were sampled inside slicks, while there was no slick present at Site H_12.

Table 3. LASER 2016 data table. Pertinent information regarding sample collection during GoMRI LASER in the Gulf of Mexico.

Site	Date	Slick present	Wind speed (m/s)	Sampling platform	SML samples taken	SSW samples taken
1	2/6/2016	No	4–5	Small boat	7	0
2	2/6/2016	No	7–8	Small boat	8	5
3	2/6/2016	No	5–7	Small boat	11	9
4	2/10/2016	No	5–7	R/V <i>F.G. Walton Smith</i>	9	3
5	2/10/2016	No	7–8	R/V <i>F.G. Walton Smith</i>	9	3
6	2/12/2016	Yes	2–3	R/V <i>F.G. Walton Smith</i>	11	8
7	2/12/2016	Yes	2–3	R/V <i>F.G. Walton Smith</i>	10	9



Figure 4. LASER 2016 sampling locations. Sampling sites and dates in the Gulf of Mexico during the 2016 GoMRI LASER research cruise. DWH refers to the Deepwater Horizon site.

3.c. DNA analysis

3.c.i. DNA extraction

DNA was extracted from the 47 mm polycarbonate membrane filters using a MoBio PowerWater DNA Isolation Kit and the associated protocol. Cells on the filter in a lysis buffer broke via vortex mixing, which isolated the microorganisms from the filter. After the protein and inhibitor removal steps, genomic DNA was collected on the silica spin column. High quality DNA was washed and eluted from the spin column for use in downstream applications (MoBio PowerWater DNA Isolation Kit Sample: Instruction Manual).

3.c.ii. Real time PCR

qPCR was used as a first step for DNA analysis to check for contamination of the samples, get initial data on *Bacillus* spp. abundance, and provide a comparison to sequencing results. The qPCR master mix contained 12.5 μL SYBR-Green 1 and 8.5 μL PCR water supplied in the FastStart Essential DNA Green Master kit (Roche Diagnostics Inc.), 1 μL of 10 μM Bac265F, and 1 μL of 10 μM Bac525R. The primers Bac265F (5'-GGCTCACCAAGGCAACGAT-3') and Bac525R (5'-GGCTGCTGGCACGTAGTTAG-3'), are designed to amplify the V3 and V4 regions of the 16S rRNA gene specific to *Bacillus* (Xiao et al. 2011), a genus well-known to contain multiple species that produce surfactants. *Bacillus* genus was also chosen because it was not found on the control filters of Kurata et al. (2016) and Hamilton (2015a,b) and so was not thought to be a persistent contaminant. Non-template controls (NTC) were used in qPCR and sequencing as a reference point for procedural contamination.

The qPCR protocol had an initial denaturing step of 95°C for 15 min, followed by 25 cycles of 94°C for 30 s, 62°C for 30 s, and 72°C for 2 min, followed by an extension at 72°C for 10 min, and finished with a melt curve. Each sampling day was analyzed in a separate qPCR run (Table2). qPCR runs for Sites 2-5 contained 2.5 μL of DNA, while

Sites 6 and 7 contained only 2 μ L of DNA. All samples were run in duplicate on a LightCycler96 (Roche Diagnostics Inc).

The threshold was set at fluorescence of 1.5 relative fluorescence units, which was in the linear phase of amplification in order to determine CT (Figure 3). Relative abundance was calculated using the PffafI method (PffafI et al. 2001):

$$ratio = \frac{E_x^{\Delta CT \text{ target (control-sample)}}}{E_{NTC}^{\Delta CT \text{ ref (control-sample)}}} \quad (1)$$

This method is similar to the $\Delta\Delta$ CT method of Livak and Schmittgen (2001), but also takes into account the efficiency of the PCR reactions, since they often differ between samples and runs (Table 4). A reaction with 100% efficiency has a value of 2, which relates to the fact that each target of double-stranded DNA should amplify into two copies of the target strand at the end of each cycle. Confidence intervals were calculated at 70% using Student's distribution coefficient, due to small sample size ($N < 30$).

3.c.iii. Sequencing

Twenty microliters of DNA from each sample were sent to ANL for amplification and sequencing. The 16S rRNA gene was targeted and amplified using primers 515F and 806R. The ANL amplification protocol had an initial denaturing step of 94 °C for 3 min, followed by 35 cycles of 94°C for 45 s, 50°C for 60 s, and 72 C for 90 s, and finished with an extension at 72°C for 10 min. Sequencing at ANL occurred via the Illumina MiSeq platform on a 151 bp x 12 bp x 151 bp MiSeq run using customized primers (Caporaso et al. 2012). Sequences were analyzed using QIIME version 1.9.1. Paired ends were joined, demultiplexed, and quality filtered. Sequences were clustered into OTUs, which were defined as $\geq 97\%$ 16S rRNA gene sequence similarity, using *de novo* interface with Greengenes version 13.5 (McDonald et al. 2012). Paired ends were joined, demultiplexed and quality filtered. Sequences were cluster into OTUs, which were defined as $\geq 97\%$ similarity.

Surfactant-associated genera, including *Bacillus*, *Pseudomonas*, *Corynebacterium*, *Acinetobacter*, *Enterobacter*, *Halomonas*, *Rhodococcus*, *Marinobacter*, *Micrococcus*, and *Arthrobacter*, were filtered from the OTU table and relative abundance was calculated. While not all species within these genera are associated with surfactants, it is not always possible to resolve sequencing datasets down to the species level. Outliers were not removed from analysis.

Confidence intervals for absolute abundance were calculated at 70% using a two-tailed t-test, Gaussian distribution and Student's distribution coefficient, due to small sample size ($N < 30$). Due to the difference in definition of confidence intervals by various authors, the Gaussian distribution is considered conservative. Confidence intervals were also calculated using Poisson distribution (see Supplementary Materials), which may be a less conservative method for this study.

4. Results and discussion

4.a. SAR overpass

The sampling conducted on February 12 during LASER occurred several hours after a TerraSAR-X satellite overpass. The TerraSAR-X stripmap intensity image shows an area 30 km wide by 50 km long with single polarization (VV) and an incidence angle of 31.06 degrees (Figure 5) (Terrasar-x.dlr.de). It was taken during an ascending pass while looking right. There was a well-defined convergence zone in the sampling area on February 12, appearing as the linear dark elongated area indicated by the white arrow in the middle of the SAR image (Figure 5B). Convergence zones associated with downwelling are known for the accumulation of organic matter and microbial life (Espedal and Johannessen, 1996). The lighter area at the bottom of the SAR image is rougher water surface, also indicating the presence of atmospheric convective cells due to warmer temperature on the southern side of the front. Oil rigs are visible in this image as bright spots.

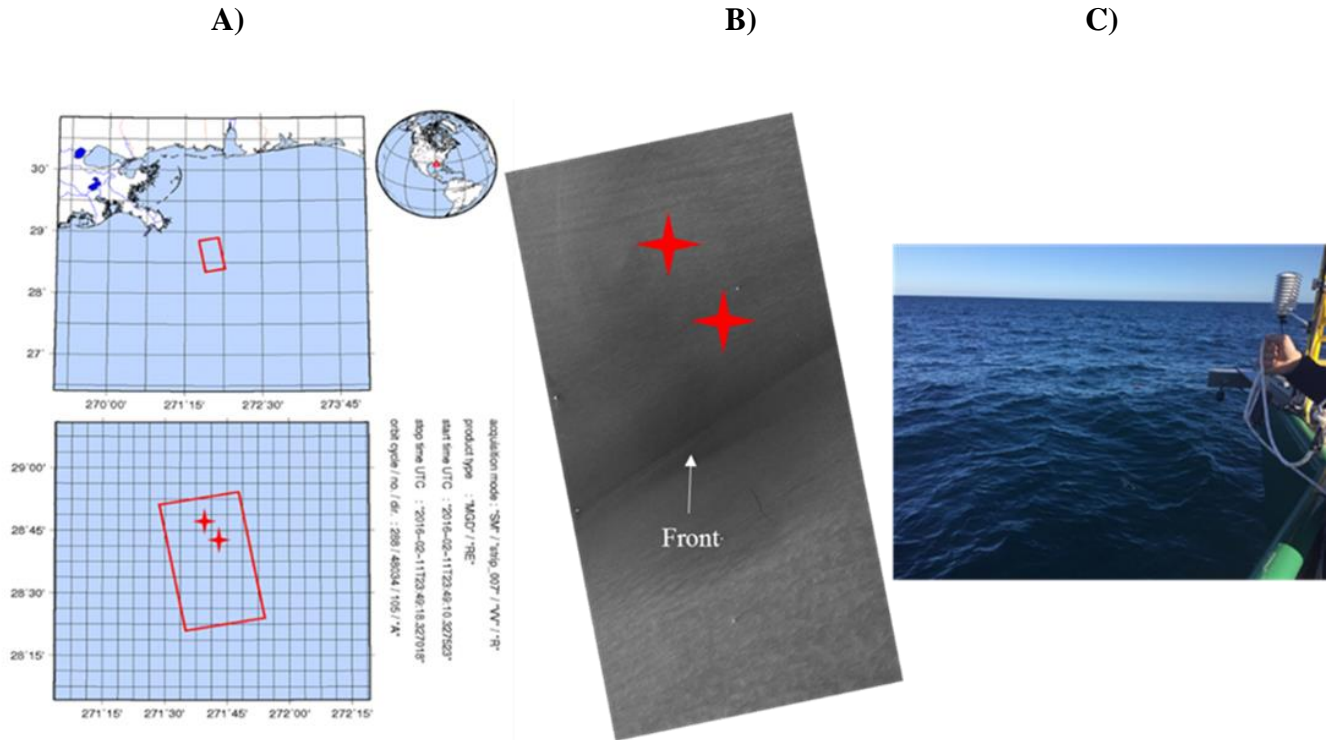


Figure 5. SAR results LASER 2016. A) Reference map and B) TerraSAR-X image acquired on February 11, 2016, at 23:49:10 UTC with sampling sites 6 and 7 denoted by red stars. The dark elongated area and surrounding dark areas in the middle of the SAR image show the slick. C) Photograph of the intermittent slick on February 12.

4.b. qPCR

4.b.i. LASER 2016

Table 4 shows the average efficiencies of each qPCR run. The Pfaffl (2001) method includes the efficiencies of the reactions when calculating relative abundance. Efficiency (E) is calculated as:

$$E = 10^{\left(-\frac{1}{\text{slope}}\right)} \quad (2)$$

where slope is provided for each sample by the LightCycler 96 software. Efficiencies can exceed two due to the presence of inhibitors, such as excess DNA, ethanol, and

secondary metabolites, as well as inadequate primer design and inaccurate pipetting (<http://www.thermofisher.com>).

Table 4. qPCR efficiencies. Sites contained in each qPCR run and reaction efficiencies \pm one standard deviation.

qPCR Run	Sites in Run	Average Efficiency
KH14	6, 7	2.28 ± 0.29
KH10	4, 5	2.50 ± 0.34
KH09	2, 3	2.54 ± 1.17

The qPCR results in Figure 6 show the differences in relative abundance of *Bacillus* spp. between the SML and SSW. Site 1 was removed from analysis because only SML samples were taken at that location (no SSW data were available for comparison). In Figure 6, red represents the SML and blue represents the SSW. The 70% confidence intervals, calculated using the Student's distribution coefficient and two-tailed t-test, are shown. Sites 3, 4, 5, and 6 showed a statistically significant difference in the relative abundance of *Bacillus* spp. between the SML and SSW. There was no statistically significant difference between SML and SSW in Site 2 and in Site 7, which were sampled under moderate wind speed conditions with no visible slick and under low wind speed conditions with a visible slick, respectively.

Samples in Sites 3 and 4 were collected under wind speeds of 5–7 m/s and there were no visible slicks. On average, these samples showed higher relative abundance of *Bacillus* spp. in the SML compared to SSW. Site 5, with wind speeds of 7–8 m/s and no visible slicks, showed more *Bacillus* spp. in the SSW compared to SML. Sites 4 and 5 were sampled in brown water of the Mississippi River plume, which could account for the larger relative abundance of *Bacillus* spp. for both SML and SSW (Figure 6). Site 6 with wind speeds of 2–3 m/s had a visible slick and showed higher relative abundance of *Bacillus* spp. in the SSW compared to the SML.

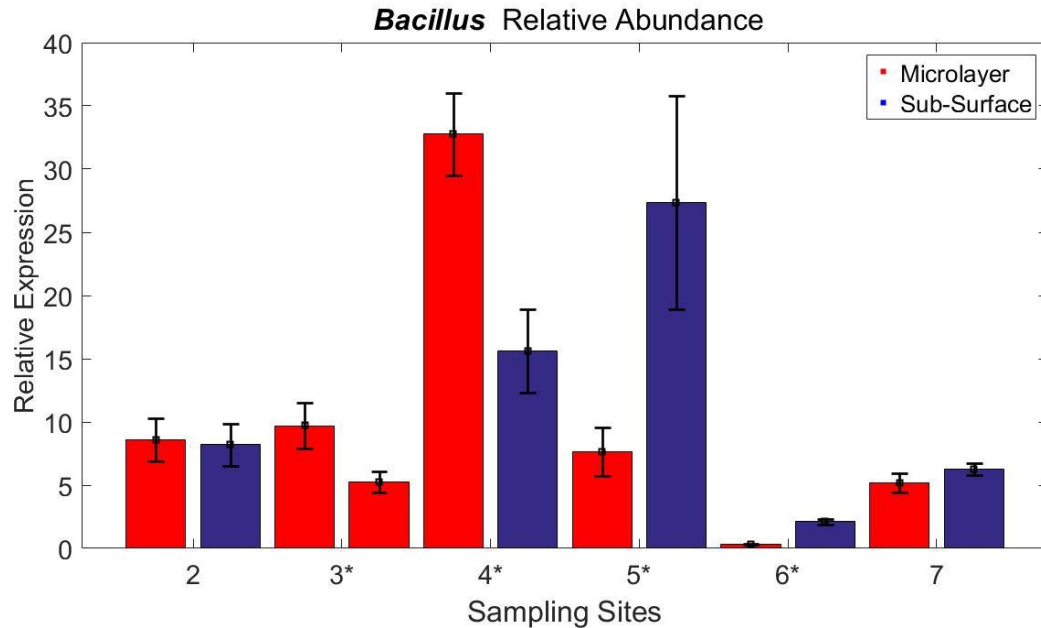


Figure 6. LASER 2016 qPCR results. Relative expression of *Bacillus* from samples collected in the Gulf of Mexico during the LASER 2016 research cruise. Y-axis is relative abundance. An asterisk (*) next to the site number indicates statistical significance.

There was considerable variation in *Bacillus* spp. abundance for both the SML and SSW samples, similar to that observed in the previous work of Hamilton et al. (2015a). In this study, the number of successive SML samples was increased from the four to six in Kurata et al. (2016) and Hamilton et al. (2015a) to as many as ten, which contributed to more robust statistics. A further increase of the number of successive samples above ten is not always feasible, because the ship drifts and often leaves the slick area before completing the sampling set.

Bacillus abundance was, in general, larger under low rather than moderate wind speed conditions. Our results suggest that under low wind speed conditions, more *Bacillus* spp., a well-known surfactant-associated bacteria, are present in the SSW compared to the SML. This conclusion is consistent with observations by Kurata et al. (2016) and Hamilton et al. (2015a, b). This indicates that surfactants may be produced in SSW and transported to the SML via physical processes such as advection, bubble

scavenging, and convection, accumulating on and enriching the sea surface microlayer, which is consistent with Cunliffe et al. (2010).

4.b.ii. SCOPE 2013

Relative abundance determined by qPCR and calculated in Hamilton et al. (2015a, b) for the samples collected during SCOPE in 2013 in the Gulf of Mexico did not yield a statistically significant difference between SML and SSW at 70% for Site H_11 or H_12 (Figure 7). However, the analysis of Site H_13, which was sampled under low wind speed, slick conditions, showed statistically significant differences between the SML and SSW at 70% and indicated that there was a higher abundance of *Bacillus* in the SML compared to SSW (Figure 8).

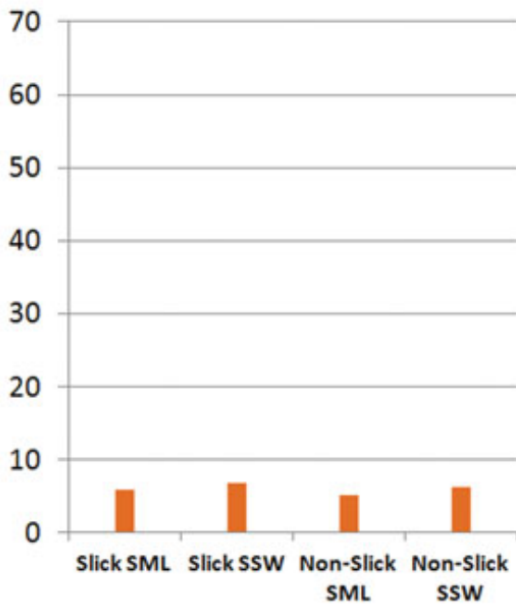


Figure 7. SCOPE 2013 qPCR results for 12/11/13. qPCR results depicting relative abundance of *Bacillus* from samples collected on December 11, 2013 (from Hamilton et al. 2015a). Y-axis is relative abundance.

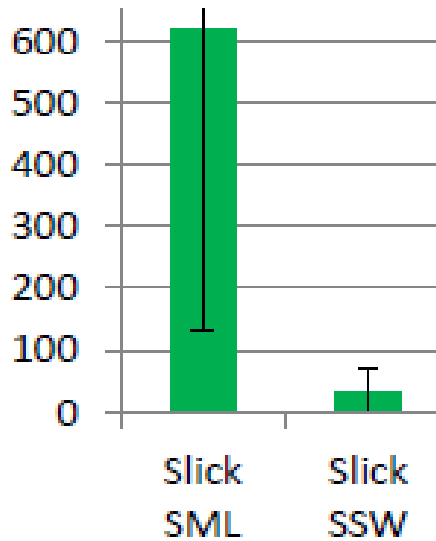


Figure 8. SCOPE 2013 qPCR results for 12/16/13. qPCR results depicting relative abundance of *Bacillus* from samples collected on December 16, 2013 (from Hamilton et al. 2015b). Y-axis is relative abundance.

4.c. Sequencing

4.c.i. LASER 2016

Over 1000 bacterial genera were identified from 181,977 OUT IDs using *de novo* OTU picking at 97% similarity. Sequencing results by site are depicted in Figure 9, and show the composition of several surfactant-associated bacterial genera for both SML and SSW. Some bacteria listed in the legend are not present in high enough amounts to be detected in Figure 9. (For composition of results by sample, see Figures S1 through S6 in Supplementary Material.) When other surfactant-associated genera are included in addition to *Bacillus* in analysis, there was a higher relative abundance of total surfactant-associated bacteria in the SSW for Sites 2, 3, 5, while there was a higher relative abundance of those bacteria in the SML for Sites 4, 6, and 7.

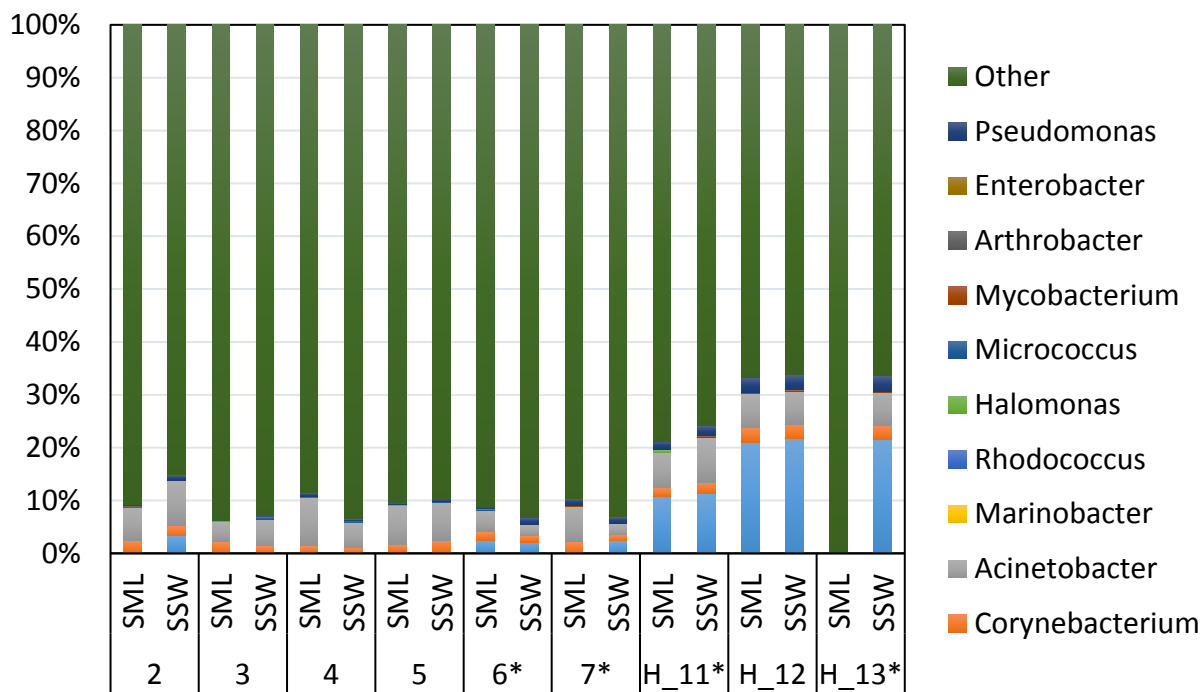


Figure 9. LASER 2016 and SCOPE 2013 relative abundance by sequencing. Relative abundance of several surfactant-associated bacterial genera in Sites 2-7 from LASER 2016 and Sites H_11- H_13 from SCOPE 2013. Y-axis is relative abundance.

There were variations in relative abundance of *Bacillus* spp. between the SML and SSW and between sites. Sites 2 and 7 showed higher relative abundance of *Bacillus* spp. in the SSW, while Sites 3, 4, 5, and 6 showed higher relative abundance of *Bacillus* spp. in the SML. The percentage of *Bacillus* spp. is negligible in sites 3, 4, and 5, whereas it accounts for 5% of total bacteria found in the SSW of Site 2, and less than 3% for Sites 6 and 7. Note that the relative abundance may not be directly related to the amount of surfactants produced by these bacteria, because relative abundance depends on presence of other bacteria in the sample. For this reason, the number of OTU hits may be a better measure of surfactant production by bacteria (Figure 10).

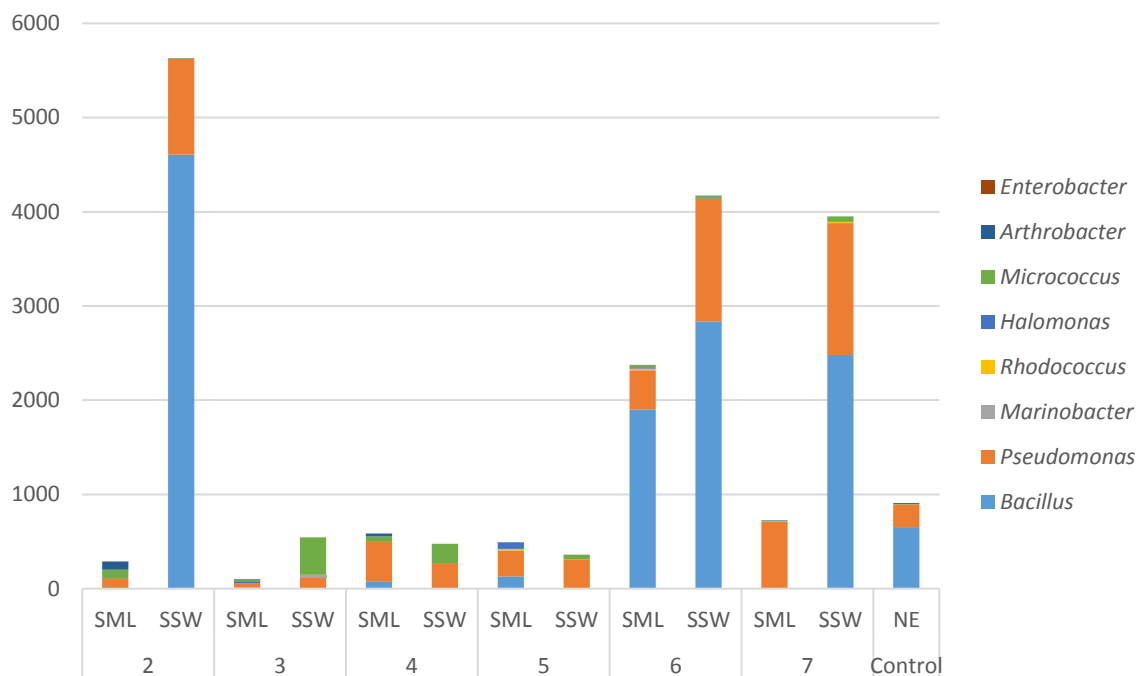


Figure 10. Average OTU hits per site. Average OTU hits per site for surfactant-associated bacterial genera.

All analyses showed high variability in OTU hits between samples taken in the same location (Figures 11-22). Due to the natural variability of microbial communities and natural sea slicks in time and space, it is necessary to estimate what is natural variation and what is contamination. An additional bar is therefore included in Figures 11-22 showing contamination levels for different surfactant-associated genera found on the NE controls. According to NE controls, the bacteria that have relatively low contamination levels include *Bacillus* (Figure 11) *Pseudomonas* (Figure 12), *Marinobacter* (Figures 15), *Rhodococcus* (Figure 16), *Halomonas* (Figure 17), *Micrococcus* (Figures 18), *Mycobacterium* (Figure 19), *Arthrobacter* (Figure 20), and *Enterobacter* (Figure 21). It should be noted that *Marinobacter*, *Rhodococcus*, *Halomonas*, *Arthrobacter*, and *Enterobacter* contain a relatively small amount of OTU hits compared to *Bacillus*, *Pseudomonas*, and *Mycobacterium*. Consequently, it is hypothesized that the main contribution to production of surfactants by bacteria comes from *Bacillus*, *Pseudomonas*, and possibly *Mycobacterium*.

Figure 11 shows total *Bacillus* average OTU hits per site. The NTC showed no presence of *Bacillus*, but some of the NE controls (average OTU hits are shown in red in Figure 11) did have *Bacillus* OTU hits. In low wind speed, slick conditions (Sites 6 and 7), *Bacillus* was more abundant in the SSW compared to the SML (Figure 11). Site 2 sampled under moderate wind speed conditions shows more OTU hits in the SSW compared to SML. In general, abundance between the SML and SSW was intermittent in moderate wind speed conditions.

Figure 12 shows total *Pseudomonas* average OTU hits per site. There was a relatively small amount of *Pseudomonas* found on the NE filters, so it is not believed to be source of contamination. Except for Sites 4 and 5, which were sampled in the brown water of the Mississippi River plume, all sites show higher abundance of *Pseudomonas* in the SSW compared to SML (Figure 12). This bacterial genus has the highest abundance among identified surfactant-associated bacteria.

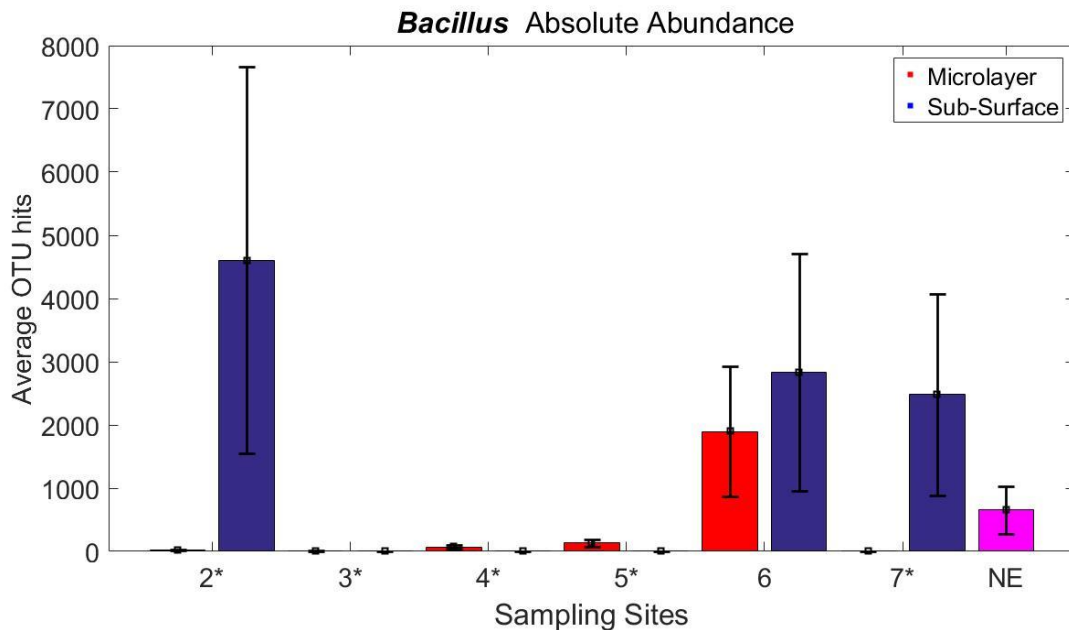


Figure 11. Average *Bacillus* OTU hits. *Bacillus* OTU hits among sites, including NE controls. An asterisk (*) next to the site number indicates statistical significance.

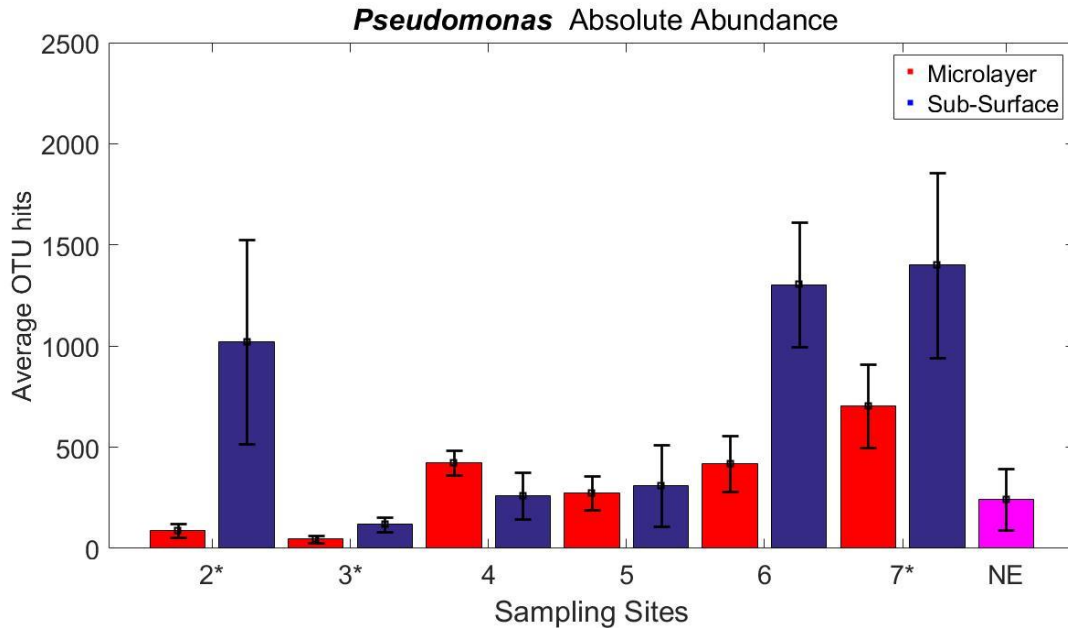


Figure 12. Average *Pseudomonas* OTU hits. *Pseudomonas* OTU hits among sites, including NE controls. An asterisk (*) next to the site number indicates statistical significance.

Figure 13 shows total *Corynebacterium* average OTU hits per site. Control NE filters indicate that there was a relatively high level of contamination from *Corynebacterium*. This genus is a known contaminant of MoBio DNA extraction kits (Glassing et al. 2016). Therefore, we cannot make any conclusions regarding the abundance of this bacterial genus, in either the microlayer or water column.

Acinetobacter also shows high levels of contamination of the NE filters (Figure 14). *Acinetobacter* is not known as a contaminant of the MoBio DNA extraction kits (Glassing et al. 2016), so this contamination may have another source. Therefore, we cannot make any definite conclusions regarding the abundance of this bacterial genus, in either the microlayer or water column.

Marinobacter was present in only the SSW of Site 3 (Figure 15). It was not found on the NE filters, indicating it is not a contaminant. Note that *Marinobacter* does not seem to be a major contributor to surfactant-production in the sites sampled in this study

due to very low abundance.

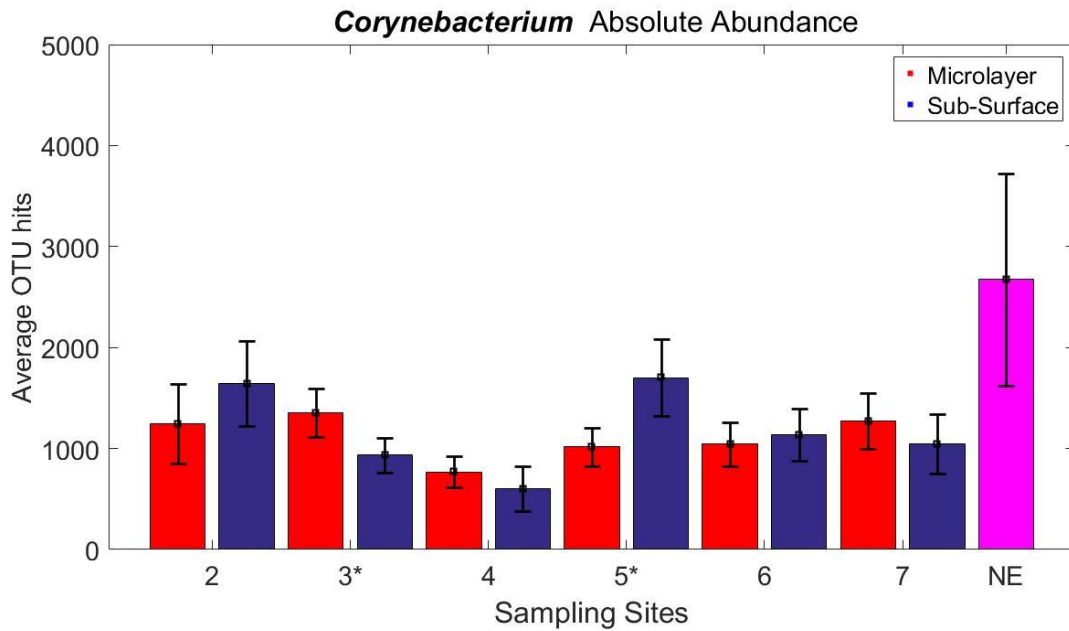


Figure 13. Average *Corynebacterium* OTU hits. *Corynebacterium* OTU hits among sites, including NE controls. An asterisk (*) next to the site number indicates statistical significance.

The abundance of *Rhodococcus* is intermittent between all sites (Figure 16). There does not appear to be a correlation between wind speed or slick conditions for the presence of this bacterial genus. The abundance of this bacteria was very low and presumably, relatively unimportant in the process of surfactant-generation.

Halomonas was consistently more abundant in the SML compared to SSW (Figure 17). It was not found on any NE filters and is therefore not considered a contaminant in this study. The abundance of this bacteria was very low and presumably, relatively unimportant in the process of surfactant-generation.

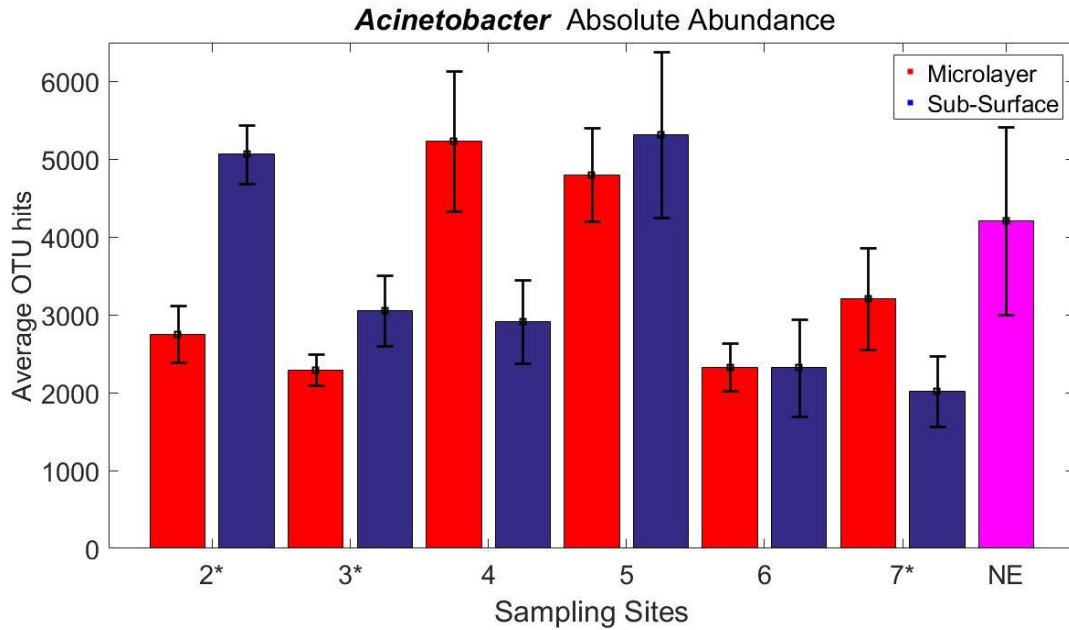


Figure 14. Average *Acinetobacter* OTU hits. *Acinetobacter* OTU hits among sites, including NE controls. An asterisk (*) next to the site number indicates statistical significance.

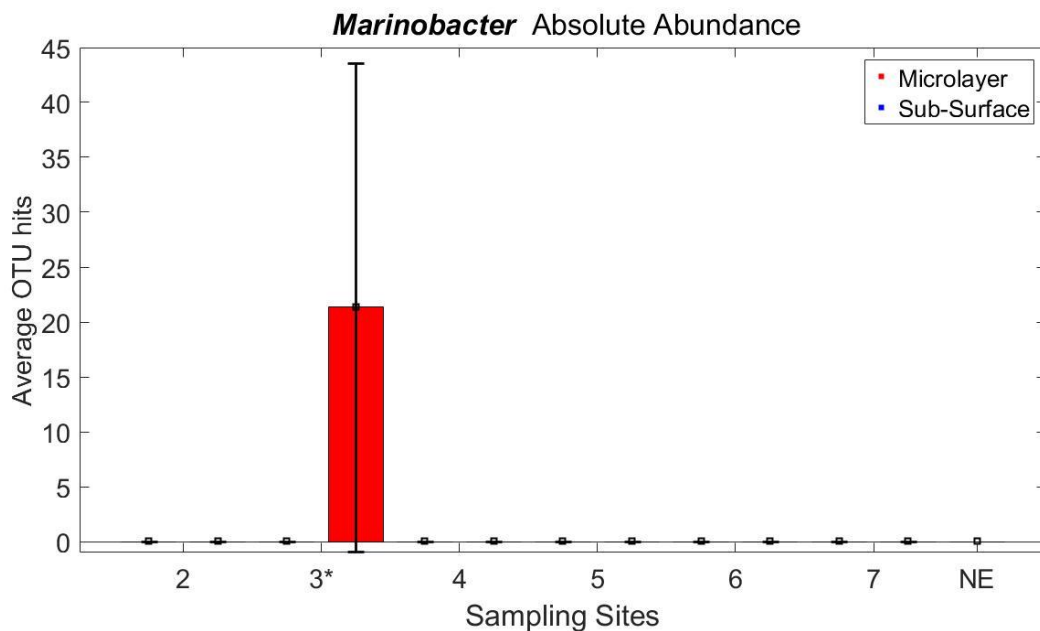


Figure 15. Average *Marinobacter* OTU hits. *Marinobacter* OTU hits among sites, including NE controls. An asterisk (*) next to the site number indicates statistical significance.

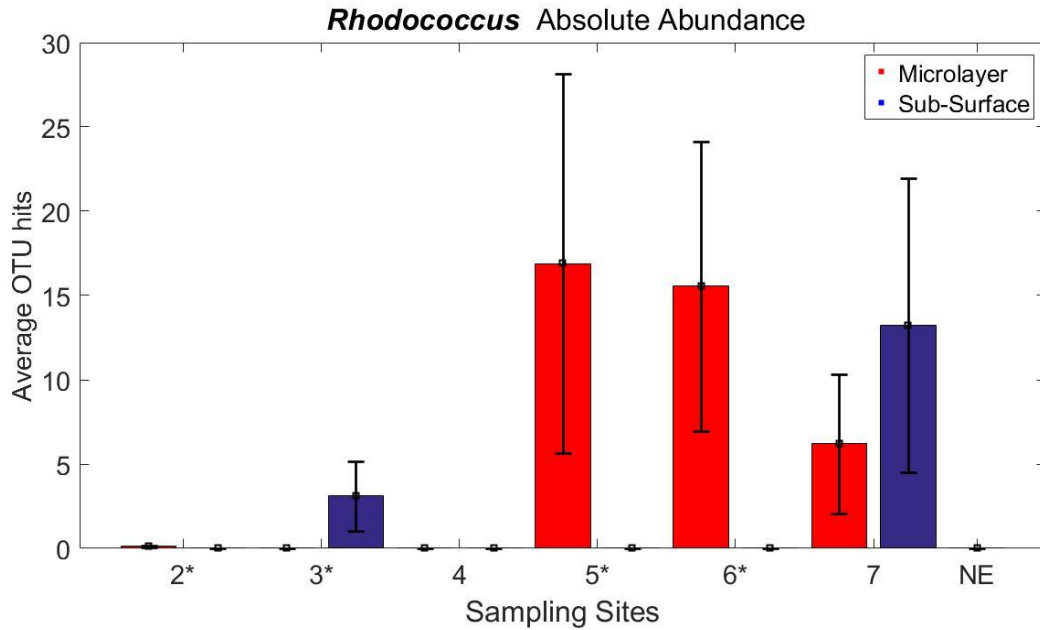


Figure 16. Average *Rhodococcus* OTU hits. *Rhodococcus* OTU hits among sites, including NE controls. An asterisk (*) next to the site number indicates statistical significance.

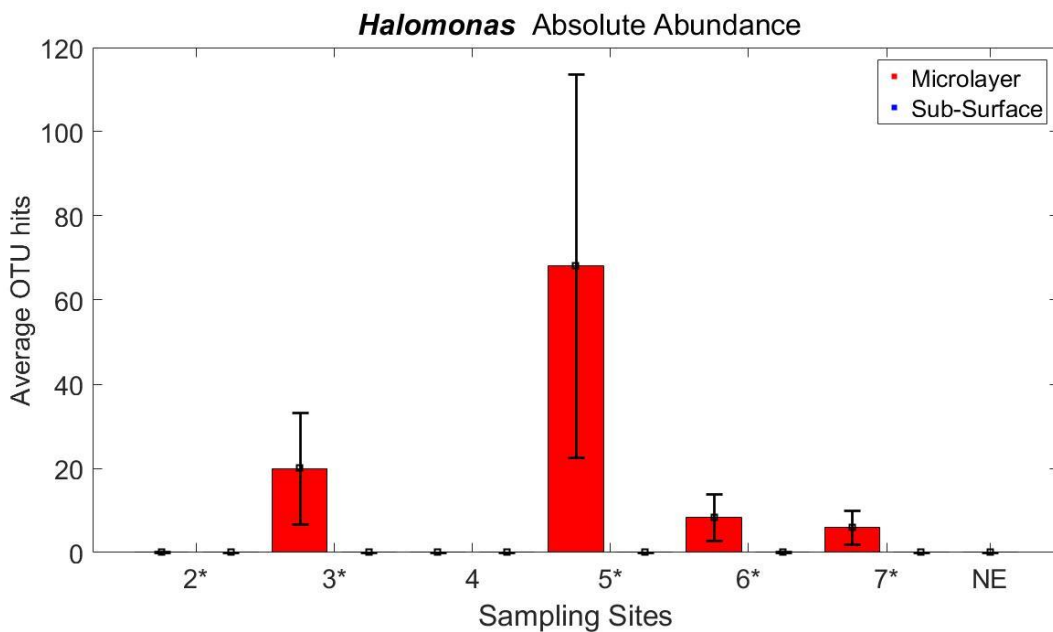


Figure 17. Average *Halomonas* OTU hits. *Halomonas* OTU hits among sites, including NE controls. An asterisk (*) next to the site number indicates statistical significance.

There does not appear to be a correlation between either wind speed or slick conditions in regards to *Micrococcus* presence in the SML versus SSW (Figure 18). The abundance of this bacteria was also relatively small, except for Site 3.

Mycobacterium showed higher abundance in the SML of slick conditions compared to the SSW of slick conditions (Figure 19). *Mycobacterium* was found on the NE controls, but was not considered a significant source of contamination.

Arthrobacter was more prevalent in the SML of all sites, except for Site 6 (Figure 20). There was detectable amounts of *Arthrobacter* on the NE filters, and may be a source of contamination. However, it is not known to be a contaminant of MoBio DNA extraction kits, so it may have another source (Glassing et al. 2016). Except for Sites 2 and 4, there was a very low abundance of *Arthrobacter*.

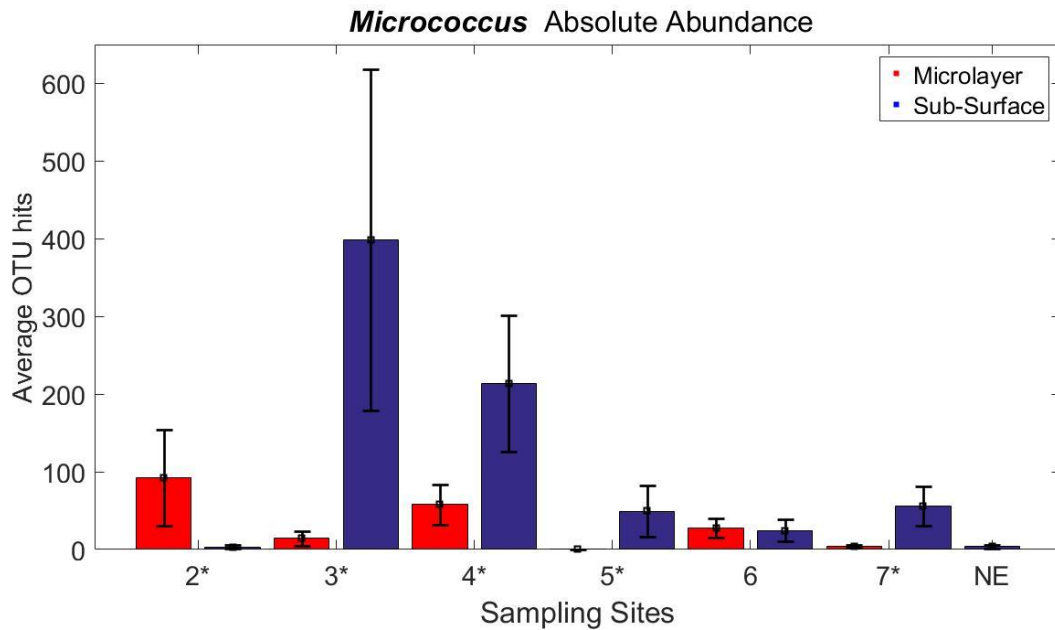


Figure 18. Average *Micrococcus* OTU hits. *Micrococcus* OTU hits among sites, including NE controls. An asterisk (*) next to the site number indicates statistical significance.

Enterobacter was detected only in a few samples in Sites 2 and 6 at very low amounts (Figure 21). Remember that averages are shown in this and the previous diagrams (Figures 11-21).

Figure 22 shows total average OTU hits per site of non-surfactant associated bacteria and unassigned bacteria. NE filters show the contamination level, which is relatively small. These bacteria also show some patterns between different sites and SML and SSW samples. In particular, they show larger abundance in SSW compared to SML for low wind speed, slick conditions in Sites 6 and 7. In brown water (Sites 4 and 5), abundance of these bacteria is slightly larger in the SML compared to the SSW.

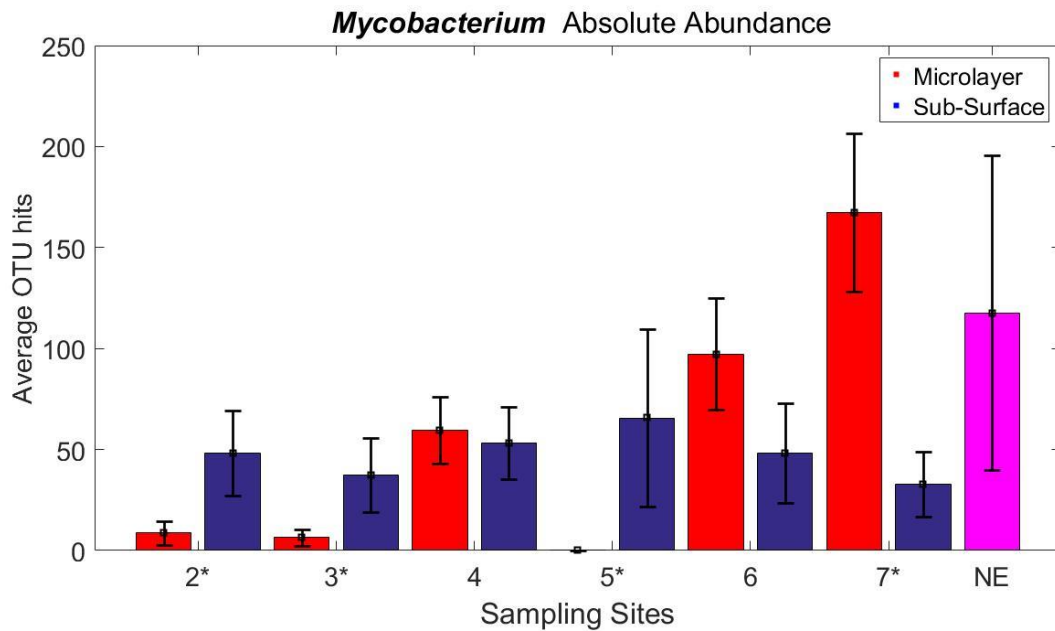


Figure 19. Average *Mycobacterium* OTU hits. *Mycobacterium* OTU hits among sites, including NE controls. An asterisk (*) next to the site number indicates statistical significance.

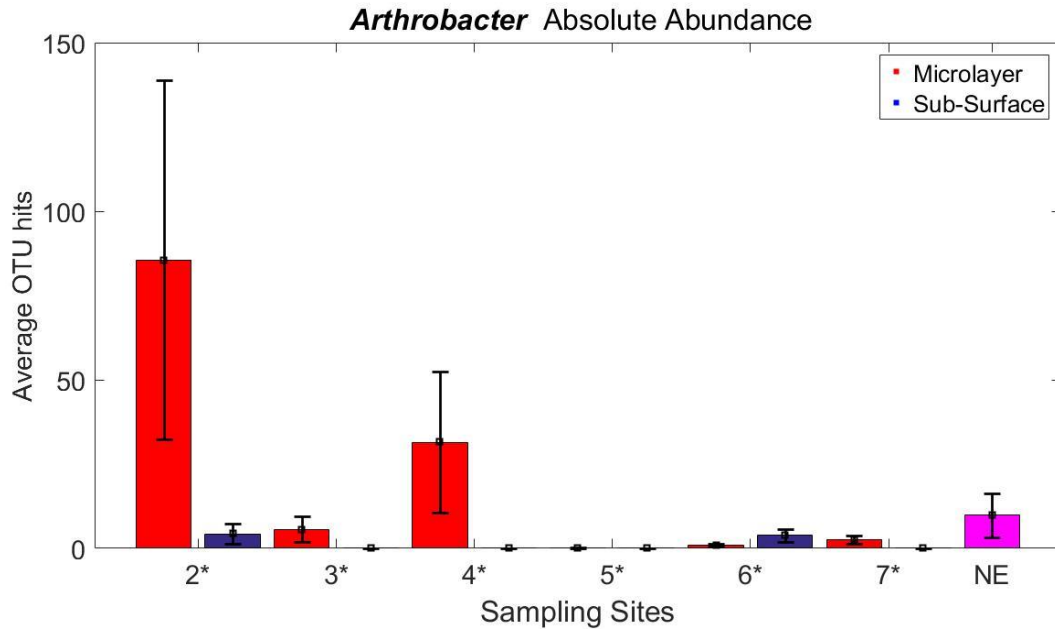


Figure 20. Average *Arthrobacter* OTU hits. *Arthrobacter* OTU hits among sites, including NE controls. An asterisk (*) next to the site number indicates statistical significance.

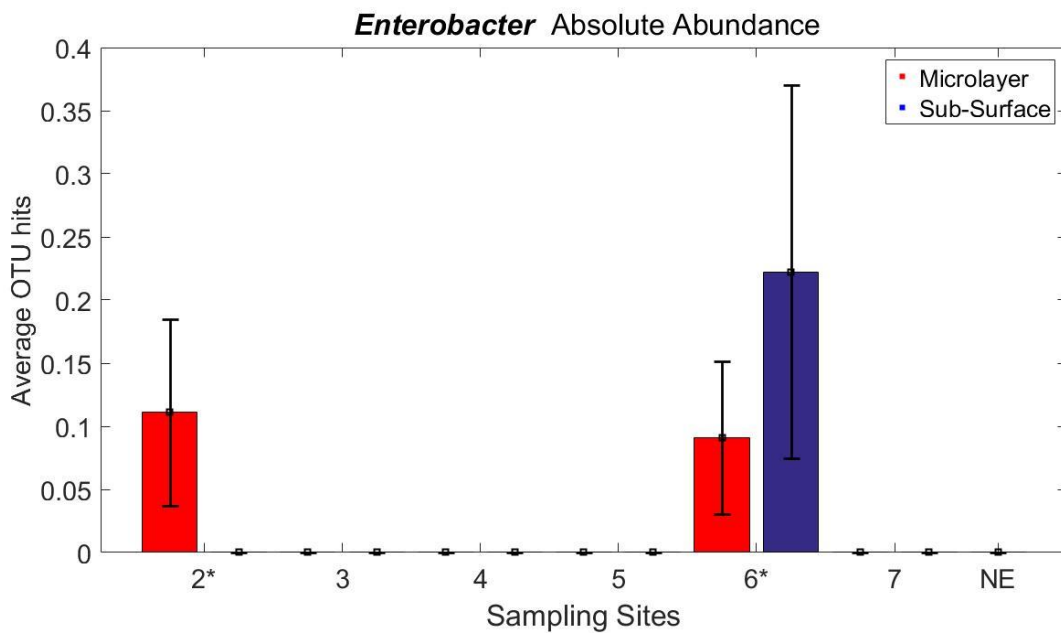


Figure 21. Average *Enterobacter* OTU hits. *Enterobacter* OTU hits among sites, including NE controls. An asterisk (*) next to the site number indicates statistical significance.

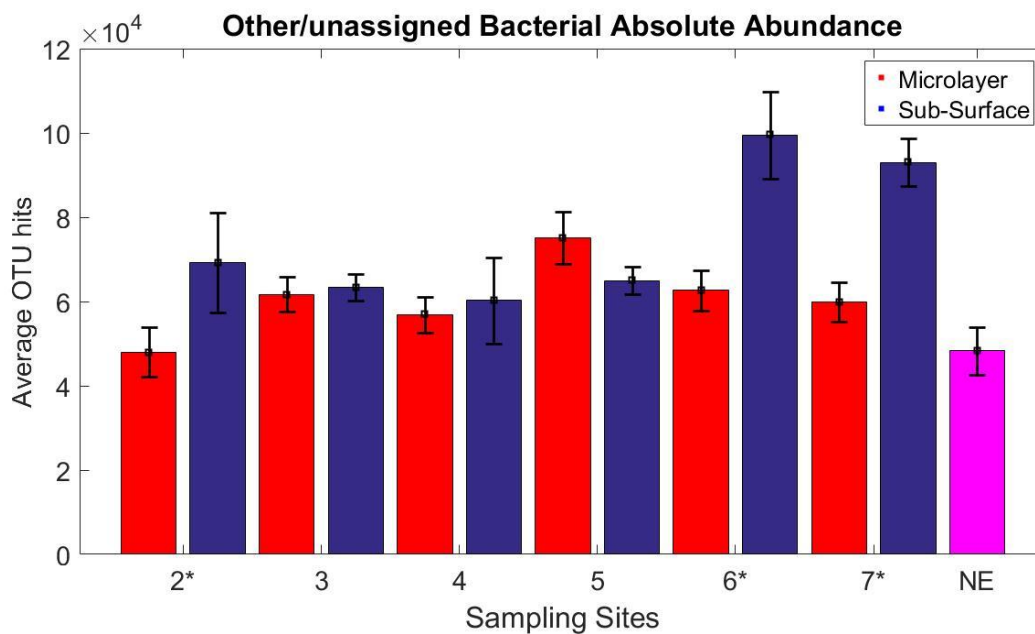


Figure 22. Total other/unassigned OTU hits. Other/unassigned OTU hits among sites, including NE controls. An asterisk (*) next to the site number indicates statistical significance.

4.c.ii. SCOPE 2013

All Sites from SCOPE 2013 indicate that there is higher relative abundance *Bacillus* spp. present in the SSW compared to the SML (see S7-S9). *Bacillus* made up approximately 11% of the bacterial composition in Site H_11 SML and SSW, and about 21% of bacterial composition of Site H_12. Site H_13 showed negligible amount of *Bacillus* in the SML, yet it made up 21% of the SSW community composition. When including additional species of surfactant-associated bacteria, there is a higher relative abundance of those bacteria in the SSW compared to SML.

4.c.iii. Contamination

Two non-exposed (NE) of seven control filters showed moderate contamination (up to an order of magnitude greater OTU hits compared to other NE control filters), while the remaining five NE controls showed negligible contamination. The air controls (AC) had

more variation in microbial community than the NE controls, which is expected. The non-template control (NTC) of autoclaved water showed no presence of *Bacillus* spp. *Corynebacterium* and *Acinetobacter* show high levels of contamination (Figures 13 and 14).

5. Conclusions

Our qPCR results suggest that under low wind speed conditions, more *Bacillus* spp., a well-known surfactant-associated bacteria, are present in the SSW compared to the SML. This conclusion is consistent with observations by Kurata et al. (2016) and Hamilton et al. (2015a, b). This indicates that surfactants may be produced in SSW and transported to the SML via physical processes such as advection, bubble scavenging, and convection, accumulating on and enriching the sea surface microlayer, which is consistent with Cunliffe et al. (2010). Sequencing analysis also suggests *Bacillus* and *Pseudomonas* are more abundant in SSW compared to SML in low wind speed, slick conditions, which is consistent with qPCR analysis. *Mycobacterium* has higher abundance in the SML compared to SSW in low wind speed, slick conditions. However, the potential contribution of *Mycobacterium* to surfactant production is expected to be relatively small because of relatively small abundance detected in these samples. All other surfactant and oil associated bacteria were identified in this study as either contaminants or occurred in very low abundance.

SAR technology can help to visualize the slick areas often related to surfactant-associated bacteria. Note that surfactant-associated bacteria may not produce any signature in ocean satellite imagery. Further research regarding pigment formation in bacteria is necessary (Pane et al. 1996) in order to adequately remotely study bacterial activity. Our results suggest that surfactant-associated bacteria mostly reside in the water column. Surfactants produced by these bacteria are transported by physical processes to the sea surface. A slick may therefore be an indication of organic material dissolved in the water column. The SAR technology can thus be implemented to track organic

material, such as dissolved oil and other pollution, in the water column by the presence of surface slicks.

In slick areas, surfactant-associated bacteria reside mostly in subsurface waters, potentially producing surfactants that could move to the surface and enrich the sea surface microlayer. This is consistent with the experimental results of other investigators (see, *e.g.*, Cunliffe et al. 2011).

6. References

- Abraham, W.R., Meyer, H., Yakimov, M. (1998) Novel glycine containing glucolipids from the alkaneusing bacterium *Alcanivorax borkumensis*. *Biochem Biophys Acta* 1393:57-62.
- Agogue, H., Casamayor, E.O., Bourrain, M., Obernosterer, I., Joux, F., Herndl, G.J., Lebaron, P. (2005) A survey on bacteria inhabiting the sea surface microlayer of coastal ecosystems. *FEMS Microbiol Ecol* 54: 269–280.
- Amann, R. I., Ludwig, W., and Schleifer, K. H. 1995. Phylogenetic identification and in situ detection of individual microbial cells without cultivation. *Microbiol. Rev.* 59, 143–169.
- Brooijmans RJW, Pastink MI, Sien RJ. 2009. Hydrocarbon-degrading bacteria: the oil-spill clean-up crew. *Microbial Biotechnology*. 2 (6): 587-594. doi:10.1111/j.1751-7915.2009.00151.x
- Caporaso JG, et al. (2011) Global patterns of 16S rRNA diversity at a depth of millions of sequences per sample. *Proc Natl Acad Sci U S A* 108 Suppl 1:4516-4522.
- Caporaso JG, Lauber CL, Walters WA, Berg-Lyons D, Huntley J, Fierer N, Owens SM, Betley J, Fraser L, Bauer M, Gormley N, Gilbert JA, Smith G, Knight R. 2012. Ultra-high-throughput microbial community analysis on the Illumina HiSeq and MiSeq platforms. *ISME J.* 6:1621–1624.
- Crow SA, Ahearn, DG, Cook, WL, and Bourquin, A.W. 1975. “Densities of bacteria and fungi in coastal surface films as determined by membrane-adsorption procedure.” *Limnol Oceanogr* 20: 602–605.
- Cunliffe M, Upstill-Goddard RC, and Murrell JC. 2011. “Microbiology of aquatic surface microlayers.” *FEMS Microbiology Reviews* 35: 233–246. DOI: 10.1111/j.1574-6976.2010.00246.x
- Cunliffe M, and Wurl O. 2014. “Guide to Best Practices to Study the Ocean’s Surface.” SCOR. Occasional Publications of the Marine Biological Association of the United Kingdom, Plymouth, UK. 118 pp.
- Dinamarca MA, Ibacache-Quiroga CJ, Ojeda JR, Troncoso JM. 2013. “Marine microbial biosurfactants: biological functions and physical properties as the basis for innovations to prevent and treat infectious diseases in aquaculture.” *Microbial Pathogens and Strategies for Combating Them: Science, Technology and Education*. FORMATEX.
- Espedal HA, and Johannessen OM. 1996. “Satellite detection of natural film on the ocean surface.” *Geophys. Res. Letters* 23: 3151-3154. DOI: 10.1029/96GL03009

- Franklin MP, McDonald IR, Bourne DG, Owens NJP, Upstill-Goddard RC, and Murrell JC. 2005. "Bacterial diversity in the bacterioneuston (sea surface microlayer): the bacterioneuston through the looking glass." *Environmental Microbiology* 7: 723–736. DOI: 10.1111/j.1462-2920.2004.00736.x
- Gade M, Byfield V, Ermakov S, Lavrova O, and Mitnik L. 2013. "Slicks as indicators for marine processes." *Oceanography* 26(2):138–149. DOI: 10.5670/oceanog.2013.39
- Glassing A, Dowd SE, Galandiuk S, Davis B, Chiodini RJ. 2016. Inherent bacterial DNA contamination of extraction and sequencing reagents may affect interpretation of microbiota in low bacterial biomass samples. *Gut Pathogens* 8:24. DOI 10.1186/s13099-016-0103-7.
- Hamilton B, Dean C, Kurata N, Vella K, Soloviev A, et al. 2015a. "Surfactant Associated Bacteria in the Sea Surface Microlayer: Case Studies in the Straits of Florida and the Gulf of Mexico." *Canadian Journal of Remote Sensing* 41(2): 135-143.
- Hamilton B. 2015b. "DNA Analysis of Surfactant Associated Bacteria in the Sea Surface Microlayer in Application to Satellite Remote Sensing Techniques: Case Studies in the Straits of Florida and the Gulf of Mexico." Dania Beach, FL: Nova Southeastern University. Available at http://nsuworks.nova.edu/cgi/viewcontent.cgi?article=1376&context=occ_stuetd.
- Harayama, S., Kasai, Y., Hara, A. (2004) Microbial communities in oil-contaminated seawater. *Current Opinion in Biotechnology* 15:205–14.
- Hardy JT. 1982. "The sea-surface microlayer: biology, chemistry and anthropogenic enrichment." *Prog Oceanogr* 11:307–328. DOI: 10.1016/0079-6611(82)90001-5
- Harvey, G.W., and Burzell, L.A. (1972) A simple microlayer method for small samples. *Limnol Oceanogr* 17: 156–157.
- Karant NGK, Deo PG, and Veena Nadig NK. 1999. "Microbial production of biosurfactants and their importance." *Current Science* 77 (1). 116-126, 166.
- Karl DM. 2007. Microbial oceanography: paradigms, processes and promise. *Microbiology* (5): 759 -769.
- Kurata N, Vella K, Hamilton B, Shivji M, Soloviev A, et al. 2016. "Surfactant-associated bacteria in the near-surface layer of the ocean." *nature.com/ScientificReports*. 6(19123). DOI: 10.1038/srep19123
- Kurata, N. (2012) Sea Surface Microlayer Microbial Observation System. Masters Thesis for Nova Southeastern University Oceanographic Center.

- Lehner S, Horstmann J, Koch W, and Rosenthal W. 1998. "Mesoscale wind measurements using recalibrated ERS SAR images" *Journal of Geophysical Research*, 103(C4): 7847-7856.
- Liss PS and Duce RA. 1997. "The sea surface and global change." Cambridge University Press, Cambridge. DOI: 10.1017/CBO9780511525025.006
- Livak KJ, Schmittgen TD (2001) Analysis of relative gene expression data using realtime quantitative PCR and the $2\Delta\Delta C(T)$ Method. *Methods* 25(4): 402–408.
- Maki, J., 1993. The air-water interface as an extreme environment. *Aquatic Microbiology: An Ecological Approach*, 409-439.
- Maneerat, S., Bamba, T., Harada, K., Kobayashi, A., Yamada, H., Kawai, F. (2006) A novel crude oil emulsifier secreted in the culture supernatant of a marine bacterium *Myroides* sp. Strain SM1. *Appl Microbiol Biotechnol* 70:254-9.
- McDonald, D., Price, M. N., Goodrich, J., Nawrocki, E. P., DeSantis, T. Z., Probst, A., et al. (2012). An improved greengenes taxonomy with explicit ranks for ecological and evolutionary analyses of bacteria and archaea. *ISME J.* 6, 610–618. doi: 10.1038/ismej.2011.139
- Mo Bio Laboratories, Inc. PowerWater DNA Isolation Kit Sample: Instruction Manual.
- Pane L, Radin L, Franconi G, Carli A. 1996. The carotenoid pigments of a marine *Bacillus firmus* strain. *Boll Soc Ital Biol Sper.* 72. 303–308.
- Perfumo, A., Banat, I.M., Canganella, F., Marchant, R. (2006) Rhamnolipid production by a novel thermotolerant hydrocarbon-degrading *Pseudomonas aeruginosa* AP02-1. *J Appl Microbiol Biotechnol* 72:132-8.
- Pffafel M. 2001. Hageleit, *Biotechnol. Lett.* 23: 275–282.
- Ponchel et al 2003. Real-time PCR based on SYBR_Freen I fluorescence: An alternative to the TaqMan assay for a relative quantification of gene rearrangements, gene amplifications, and micro gene deletions. *BMC Biotechnology* 3:18 DOI: 10.1186/1472-6750-3-18.
- Reinthal T, Sintes E, Herndl GJ. 2008. Dissolved organic matter and bacterial production and respiration in the sea surface microlayer of the open atlantic and the western Mediterranean sea. *Limnology and Oceanography*. 53: 122-136.
- Satpute SK, Banat IM, Dhakephalkar PK, Banpurkar AG, Chopade BA. 2010. "Biosurfactants, bioemulsifiers and exopolysaccharides from marine microorganisms." *Biotechnology Advances* 28, 436-450. DOI: 10.1016/j.biotechadv.2010.02.006

- Sayem, S.M.A., Manzo, E., Ciavatta, L., Tramice, A., Cordone, A., Zanfardino, A., de Felice, M., Varcamonti, M. (2011) Anti-biofilm activity of an exopolysaccharide from a sponge-associated strain of *Bacillus licheniformis*. *Microbial Cell Factories* 10, 74. 17.
- Sekhon KK, Khanna S, Cameotra SS. 2012. "Biosurfactant production and potential correlation with esterase activity." *Pet. Environ. Biotechnol.*, 3 (7). DOI: 10.4172/2157-7463.1000133.
- Sieburth, J.M. (1965) Bacteriological samplers for air-water and water-sediment interfaces. *Ocean science and Ocean engineering. Transactions of the Joint Conference, MTS and ASLO, Washington, DC*, pp. 1064-1068.
- Soloviev A, Lukas R. 2014. "The Near-Surface Layer of the Ocean: Structure, Dynamics and Application." Springer, pp 537. DOI: 10.1038/srep05306
- Soloviev AV, Gilman M, Young K, Bruschi S, Lehner S, 2010: Sonar measurements in ship wakes simultaneous with TerraSAR-X overpasses. *Geoscience and Remote Sensing, IEEE Transactions* 48, 841-851.
- Stolle C, Nagel K, Labrenz M, Jurgens K. 2010. Succession of the sea-surface microlayer in the coastal Baltic Sea under natural and experimentally induced low-wind conditions. *Biogeosciences*. 7: 2975-2988. doi:10.5194/bg-7-2975-2010
- Velotto D, Migliaccio M, Nunziata F, Lehner S. 2011. "Dual polarized TerraSAR-X data for oil-spill observation." *IEEE TGARS* 49: 4751-4762. DOI: 10.1109/TGRS.2011.2162960
- Wheeler, J. R., 1975. Formation and collapse of surface films. *Limnol. Oceanogr.* 20, 338-342.
- Whitman, W.B., Coleman D.C., Wiebe, W.J. (1998) Prokaryotes: The unseen majority. *Proceedings of the National Academy of Sciences of the United States of America*. 95:6578-6583.
- Wurl O, Wurl E, Miller L, Johnson K, Vagle S. 2011. "Formation and global distribution of sea-surface microlayers." *Biogeosciences* 8: 121-135. DOI: 10.5194/bg-8-121-2011
- Wurl, O. and Holmes, M. (2008) The gelatinous nature of the sea-surface microlayer, *Mar. Chem.*, 110, 89-97.
- Xiao Y, Zeng GM, Yang ZH, Ma YH, Huang C, Shi WJ, Xu ZY, Huan J, Fan CZ. 2011. Effects of continuous thermophilic composting (ctc) on bacterial community in the active composting process. *Microbial Ecology* 62 (3): 599-608.
- Yang B, Wang Y, Qian P. 2016. Sensitivity and correlation of hypervariable regions in 16S rRNA genes in phylogenetic analysis.

Supplementary Materials

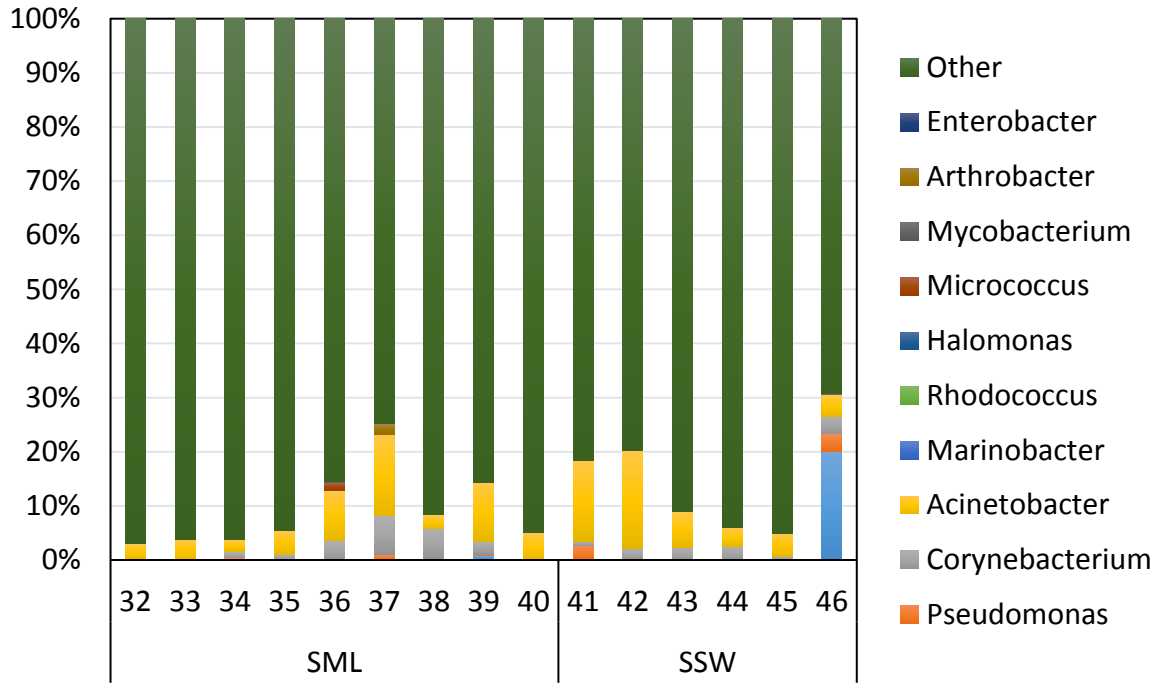


Figure S1. Relative abundance of surfactant-associated bacteria of each sample in Site 2.

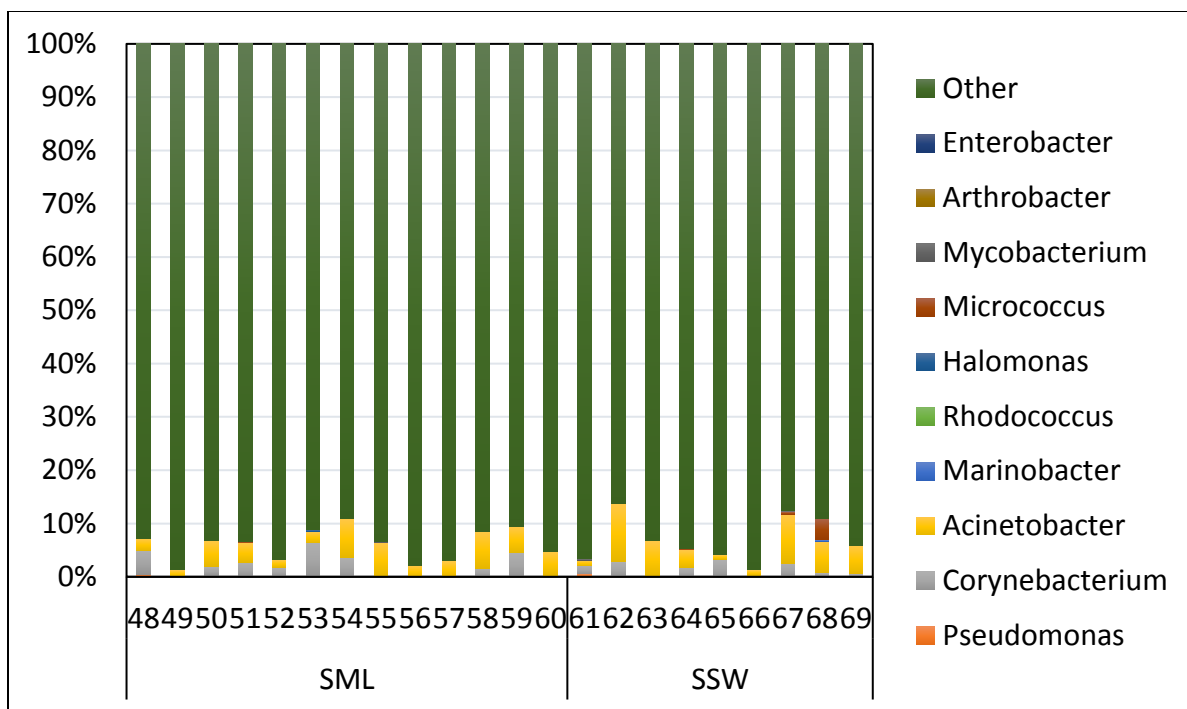


Figure S2. Relative abundance of surfactant-associated bacteria of each sample in Site 3.

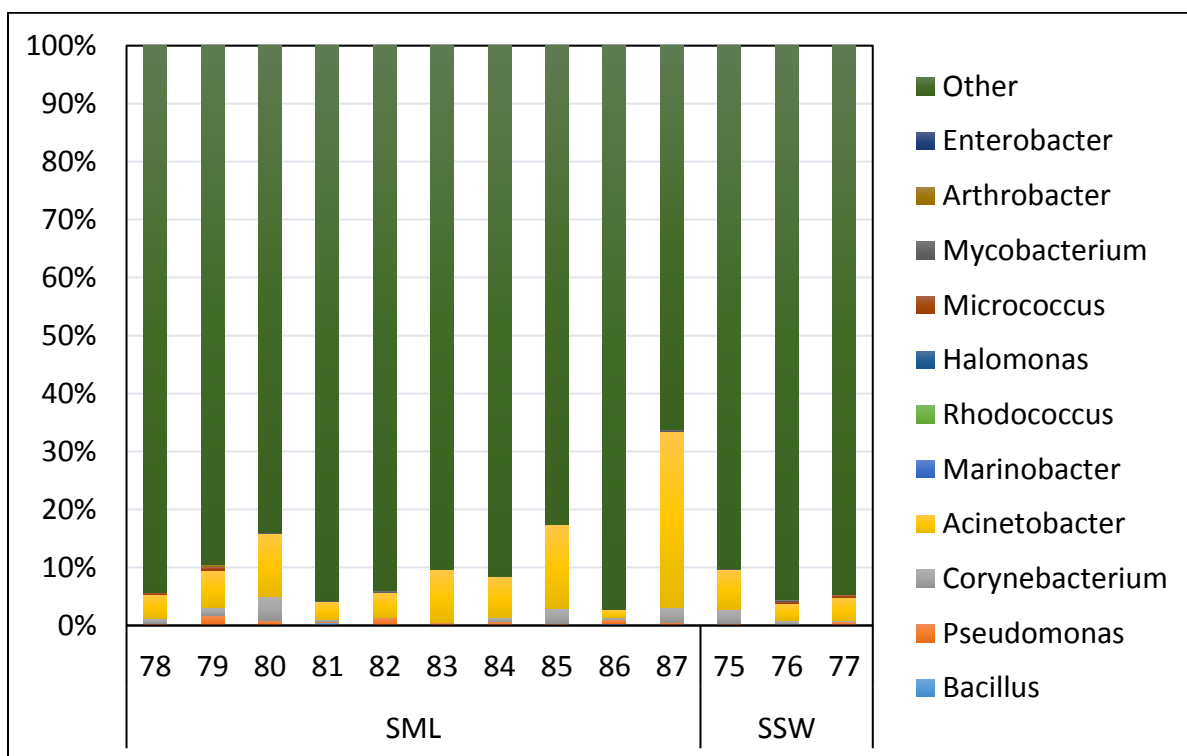


Figure S3. Relative abundance of surfactant-associated bacteria of each sample in Site 4.

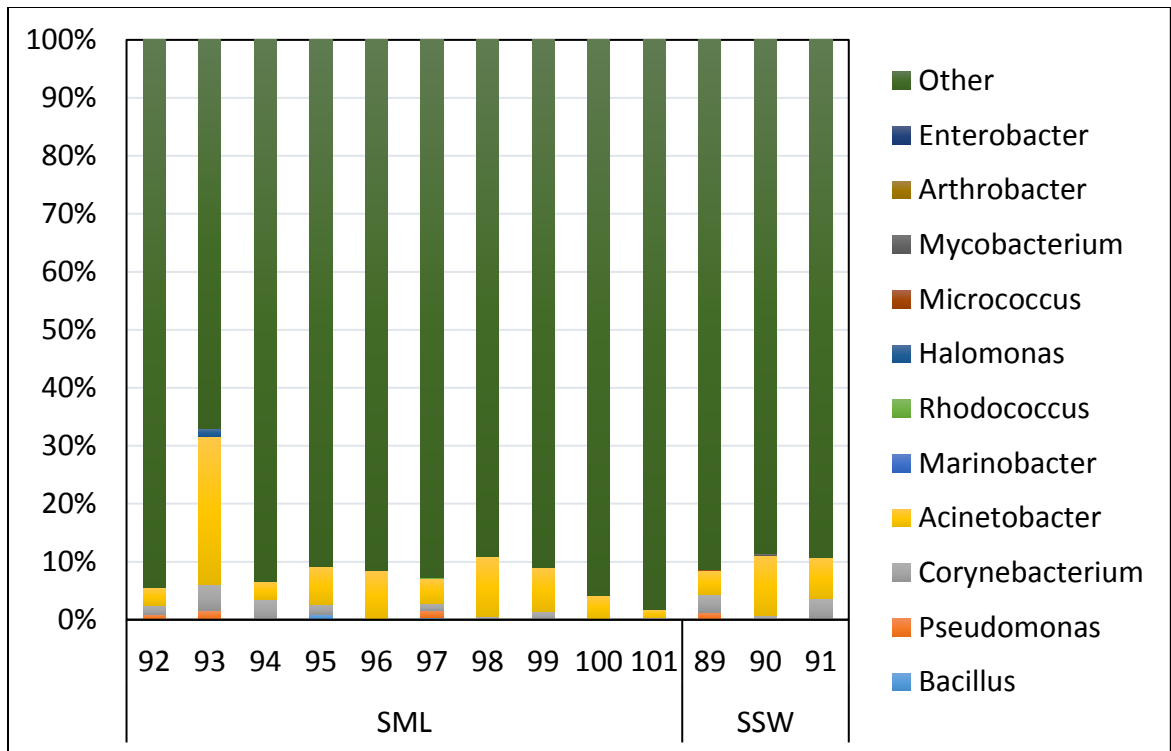


Figure S4. Relative abundance of surfactant-associated bacteria of each sample in Site 5.

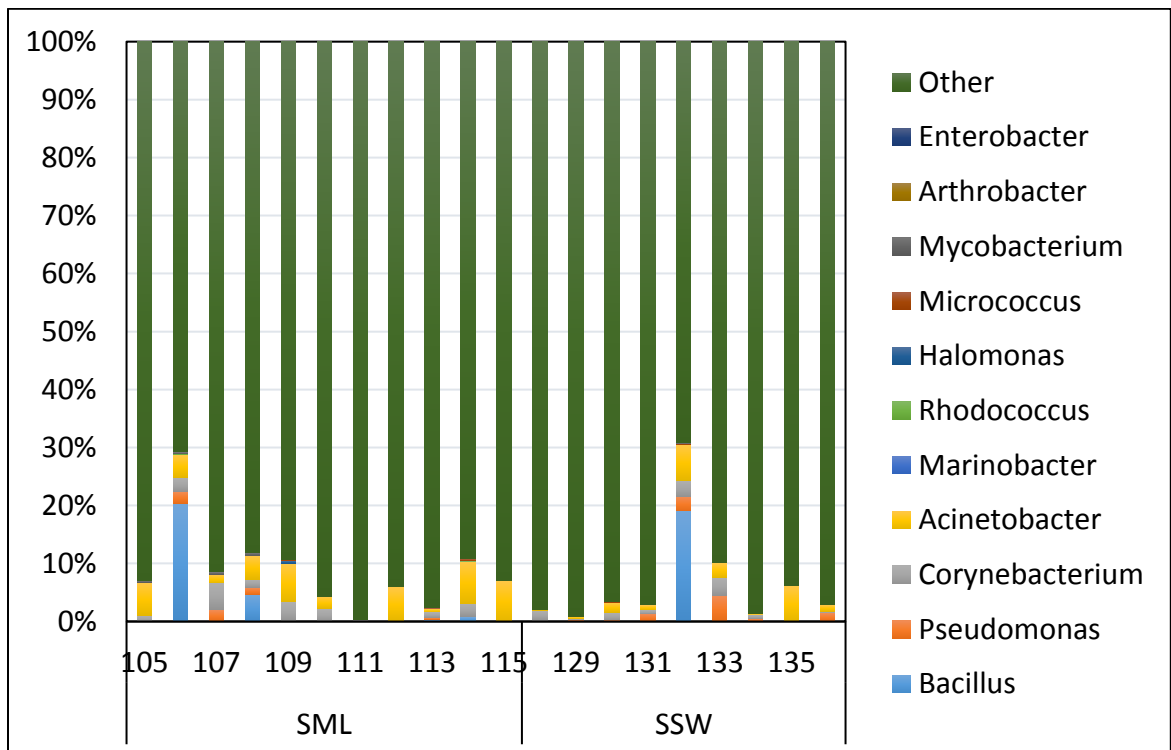


Figure S5. Relative abundance of surfactant-associated bacteria of each sample in Site 6.

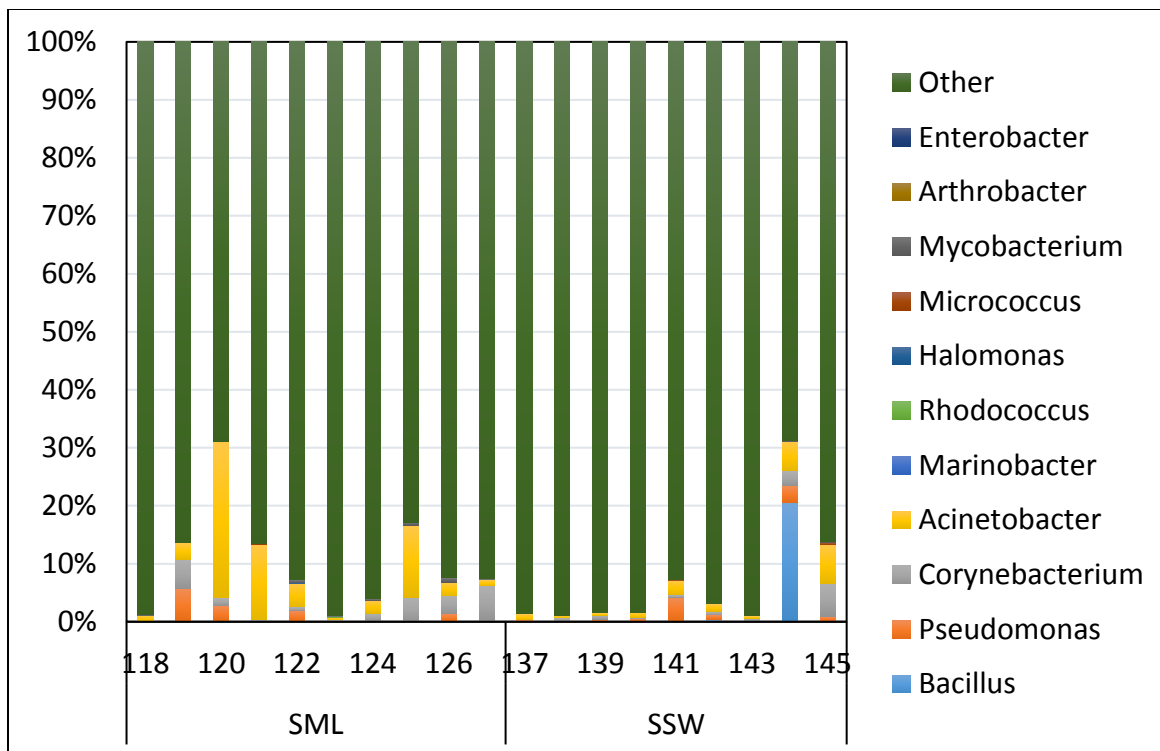


Figure S6. Relative abundance of surfactant-associated bacteria of each sample in Site 7.

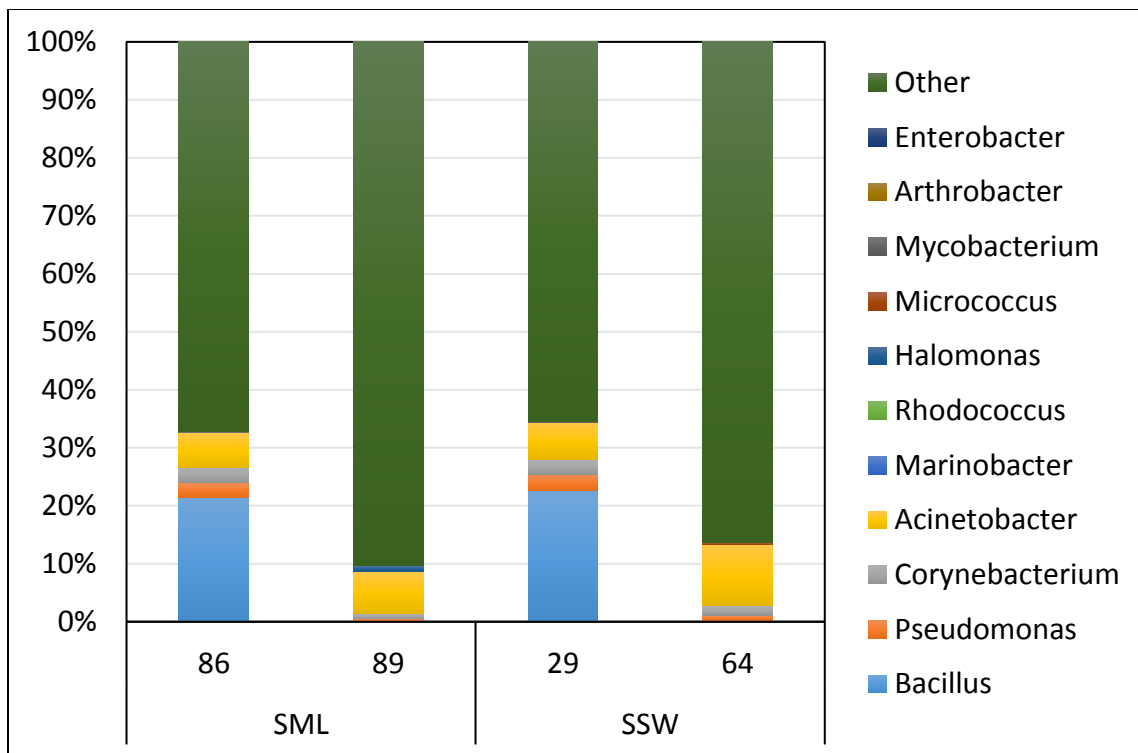


Figure S7. Relative abundance of surfactant-associated bacteria of each sample in Site H_11.

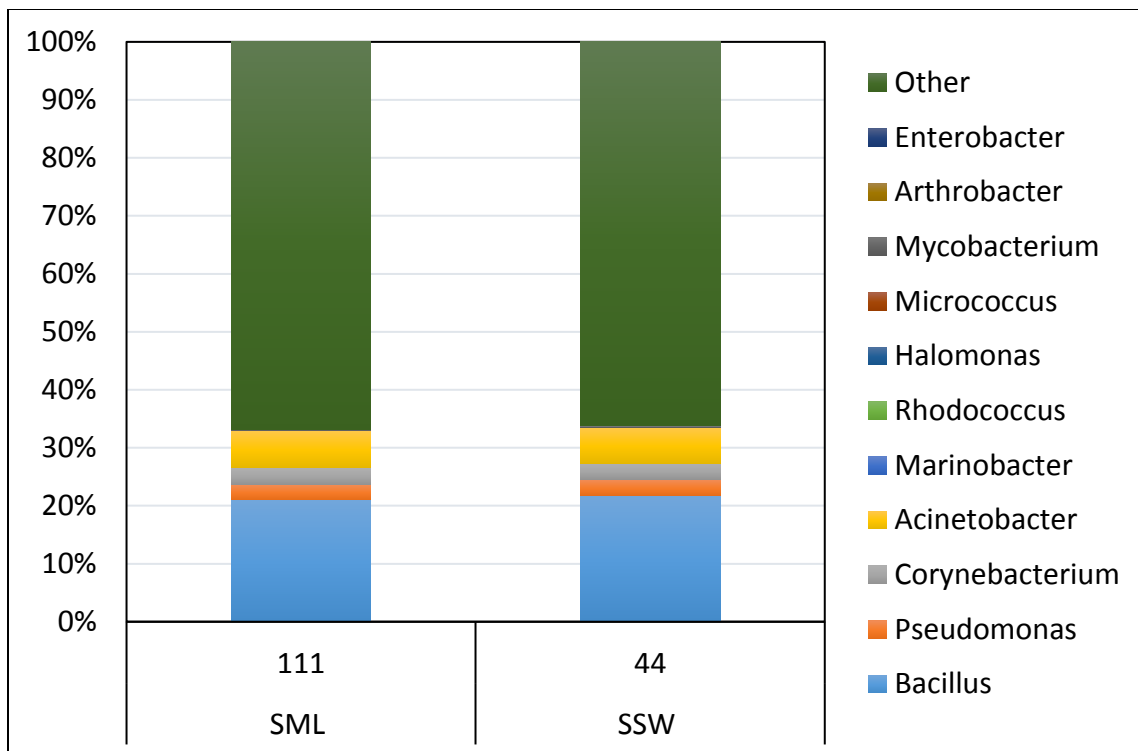


Figure S8. Relative abundance of surfactant-associated bacteria of each sample in Site H_12.

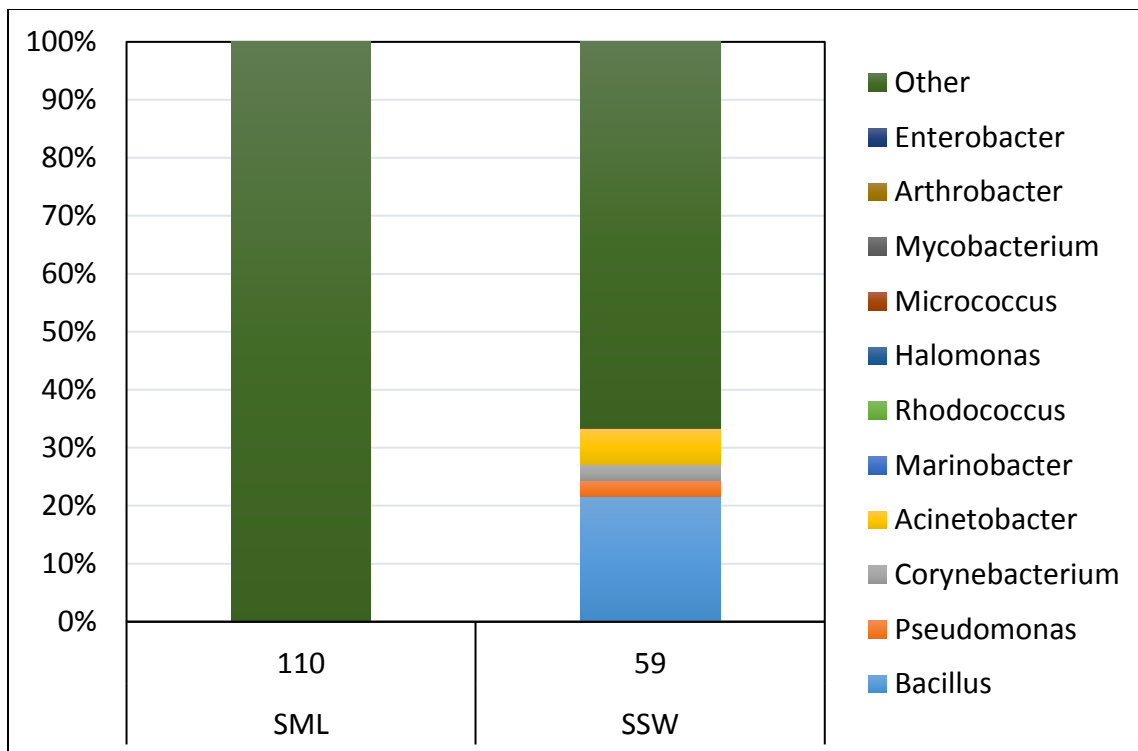


Figure S9. Relative abundance of surfactant-associated bacteria of each sample in Site H_13.

Poisson distribution with 95% confidence

The following tables show the mean (x), coefficient to calculate 95% confidence (z), and the minimum confidence interval (Min CI) and maximum confidence interval (Max CI). The top line in each site represents SML, and the bottom line for each site represents SSW. An asterisk (*) indicates statistical significance.

Table S1. *Bacillus* absolute abundance with Poisson distribution.

	x	z	Min CI	Max CI
2*	19	1.96	10.45656	27.54344
	4605.833	1.96	4472.815	4738.851
3	11.66667	1.96	4.971992	18.36134
	3.555556	1.96	0.448789	7.840412
4*	70.9	1.96	54.39638	87.40362
	3	1.96	0.163998	6.953637
5*	131.5	1.96	109.024	153.976
	1	1.96	0.060256	3.980256
6*	1898.455	1.96	1813.055	1983.854
	2835.444	1.96	2731.077	2939.812
7*	3.9	1.96	0.02931	7.77069
	2480.444	1.96	2382.828	2578.06
Control	653	1.96	602.9144	703.0856

Table S2. *Pseudomonas* absolute abundance with Poisson distribution.

	x	z	Min CI	Max CI
2*	89.44444	1.96	70.90773	107.9812
	1020.167	1.96	957.5642	1082.769
3*	46.83333	1.96	33.4201	60.24657
	118.2222	1.96	96.91113	139.5333
4*	425.1	1.96	384.6888	465.5112
	261	1.96	229.3352	292.6648
5	272.8	1.96	240.4273	305.1727
	310.3333	1.96	275.8054	344.8612
6*	419.0909	1.96	378.9664	459.2155
	1304.222	1.96	1233.439	1375.006
7*	703.8	1.96	651.8027	755.7973
	1400.444	1.96	1327.096	1473.793
NE	241.4	1.96	210.9474	271.8526

Table S3. *Corynebacterium* absolute abundance with Poisson distribution.

	x	z	Min CI	Max CI
2*	1243	1.96	1173.898	1312.102
	1642.833	1.96	1563.391	1722.276
3*	1353.833	1.96	1281.716	1425.951
	934.4444	1.96	874.5298	994.3591
4*	769.6	1.96	715.2263	823.9737
	603.3333	1.96	555.1902	651.4765
5*	1015.8	1.96	953.3316	1078.268
	1702.667	1.96	1621.79	1783.543
6	1043.818	1.96	980.4942	1107.142
	1133.556	1.96	1067.566	1199.545
7*	1273.6	1.96	1203.652	1343.548
	1045.778	1.96	982.3943	1109.161
NE	2672.2	1.96	2570.881	2773.519

Table S4. *Acinetobacter* absolute abundance with Poisson distribution.

	x	z	Min CI	Max CI
2*	2753.667	1.96	2650.815	2856.518
	5065.833	1.96	4926.331	5205.336
3*	2294.667	1.96	2200.777	2388.556
	3059	1.96	2950.596	3167.404
4*	5237.5	1.96	5095.654	5379.346
	2917	1.96	2811.142	3022.858
5*	4800.9	1.96	4665.094	4936.706
	5318.333	1.96	5175.397	5461.27
6	2329.636	1.96	2235.034	2424.238
	2323.889	1.96	2229.404	2418.374
7	3209.5	1.96	3098.461	3320.539
	2020.778	1.96	1932.67	2108.886
NE	4212.8	1.96	4085.584	4340.016

Table S5. *Marinobacter* absolute abundance with Poisson distribution.

	x	z	Min CI	Max CI
2	0	1.96	0	0
	0	1.96	0	0
3*	0	1.96	0	0
	21.333333	1.96	12.28048	30.38619
4	0	1.96	0	0
	0	1.96	0	0
5	0	1.96	0	0
	0	1.96	0	0
6	0	1.96	0	0
	0	1.96	0	0
7	0	1.96	0	0
	0	1.96	0	0
NE	0	1.96	0	0

Table S6. *Rhodococcus* absolute abundance with Poisson distribution.

	x	z	Min CI	Max CI
2	0.111111	1.96	0.046823	1.35349
	0	1.96		
3	0	1.96		
	3.111111	1.96	0.243041	7.157271
4	0	1.96	0	0
	0	1.96	0	0
5	16.9	1.96	8.842517	24.95748
	0	1.96	0	0
6	15.54545	1.96	7.817621	23.27329
	0	1.96	0	0
7	6.2	1.96	1.319639	11.08036
	13.22222	1.96	6.095197	20.34925
NE	0	1.96	0	0

Table S7. *Halomonas* absolute abundance with Poisson distribution.

	x	z	Min CI	Max CI
2	0.111111	1.96	0.046823	1.35349
	0	1.96	0	0
3	20	1.96	11.23461	28.76539
	0	1.96	0	0
4	0	1.96	0	0
	0	1.96	0	0
5	68.2	1.96	52.01367	84.38633
	0	1.96	0	0
6*	8.363636	1.96	2.695326	14.03195
	0.111111	1.96	0.046823	1.35349
7	6	1.96	1.199	10.801
	0	1.96	0	0
NE	0	1.96	0	0

Table S8. *Micrococcus* absolute abundance with Poisson distribution.

	x	z	Min CI	Max CI
2*	92.77778	1.96	73.89882	111.6567
	3.333333	1.96	0.47631	7.633218
3*	14.33333	1.96	6.912893	21.75377
	398.6667	1.96	359.5321	437.8013
4*	57.8	1.96	42.89884	72.70116
	213.6667	1.96	185.0167	242.3167
5	0	1.96	0	0
	49.33333	1.96	35.56675	63.09992
6	27.72727	1.96	17.40656	38.04798
	24.44444	1.96	14.75395	34.13494
7*	4.2	1.96	0.183195	8.216805
	55.44444	1.96	40.85008	70.03881
NE	3.8	1.96	0.769544	8.411031

Table S9. *Mycobacterium* absolute abundance with Poisson distribution.

	x	z	Min CI	Max CI
2*	8.777778	1.96	2.970824	14.58473
	48.33333	1.96	34.70699	61.95968
3*	6.416667	1.96	1.451763	11.38157
	37.44444	1.96	25.45084	49.43805
4	59.5	1.96	44.3813	74.6187
	53.33333	1.96	39.01952	67.64715
5*	0	1.96	0	0
	65.66667	1.96	49.78381	81.54952
6*	97.27273	1.96	77.94185	116.6036
	48.33333	1.96	34.70699	61.95968
7*	167.4	1.96	142.0409	192.7591
	32.66667	1.96	21.46433	43.869
NE	117.6	1.96	96.34507	138.8549

Table S10. *Arthrobacter* absolute abundance with Poisson distribution.

	x	z	Min CI	Max CI
2*	85.55556	1.96	67.42629	103.6848
	4.333333	1.96	0.253268	8.413399
3	5.666667	1.96	1.000933	10.3324
	0	1.96	0	0
4	31.5	1.96	20.49953	42.50047
	0	1.96	0	0
5	0.1	1.96	0.039011	1.278624
	0	1.96		
6	1	1.96	-0.42719	3.518817
	3.888889	1.96	0.612762	8.774317
7	2.6	1.96	-0.00159	6.293217
	0	1.96	0	0
NE	9.8	1.96	3.664229	15.93577

Table S11. *Enterobacter* absolute abundance with Poisson distribution.

	x	z	Min CI	Max CI
2	0.111111	1.96	0.046823	1.35349
	0	1.96	0	0
3	0	1.96	0	0
	0	1.96	0	0
4	0	1.96	0	0
	0	1.96	0	0
5	0	1.96	0	0
	0	1.96	0	0
6	0.090909	1.96	0.032758	1.214683
	0.222222	1.96	-0.11269	1.73522
7	0	1.96	0	0
	0	1.96	0	0
NE	0	1.96	0	0

Table S12. Other/unassigned absolute abundance with Poisson distribution.

	x	z	Min CI	Max CI
2*	47951.56	1.96	47808.49	48094.62
	69280.17	1.96	69069.55	69490.78
3*	61668.42	1.96	61527.91	61808.92
	63397	1.96	63232.5	63561.5
4*	56931.9	1.96	56784.01	57079.79
	60263.33	1.96	59985.54	60541.13
5*	75045	1.96	74875.21	75214.79
	64995	1.96	64706.51	65283.49
6*	62646.82	1.96	62498.9	62794.73
	99542.22	1.96	99336.09	99748.35
7*	59923.1	1.96	59771.38	60074.82
	93027.56	1.96	92828.29	93226.82
NE	48313.4	1.96	48120.73	48506.07